UNIVERSITY OF CALIFORNIA
RIVERSIDE

CaMKKβ/AMPK Negatively Regulates Adiposity

A Dissertation submitted in partial satisfaction
of the requirements for the degree of

Doctor of Philosophy

in

Biochemistry and Molecular Biology

by

I-Chen Peng

December 2011

Dissertation Committee:

Dr. John Y-J. Shyy, Chairperson
Dr. Jolinda Traugh
Dr. Kathryn Defea

The Dissertation of I-Chen Peng is approved:

Committee Chairperson

University of California, Riverside

Acknowledgements

I would like to thank my research advisor Dr. John Y-J. Shyy for his guidance, support and encouragement to help me accomplish my research work here. I would also like to thank Dr. Jolinda Traugh, Dr. Kathryn Defea, and Dr. David Johnson for their time, suggestions and valuable comments for my work and dissertation. I am thankful to all of my colleagues and friends for their generous help and precious suggestions.

Finally, I would like to thank my parents for their endless love, care and support.

ABSTRACT OF THE DISSERTATION

CaMKKβ/AMPK Negatively Regulates Adiposity

by

I-Chen Peng

Doctor of Philosophy, Graduate Program in
Biochemistry and Molecular Biology
University of California, Riverside, December 2011
Dr. John Y-J. Shyy, Chairperson

Lipid synthesis and storage in adipose tissues contribute to energy homeostasis, which is inversely regulated by activated AMP-activated protein kinase (AMPK). Here, I report that Ca^{2+}/calmodulin-dependent protein kinase kinase β (CaMKKβ) negatively regulates lipogenesis in adipocytes through its phosphorylation of AMPK. Specifically, the glucagon-activated CaMKKβ/AMPK cascade inhibits acetyl-CoA carboxylase (ACC) activity through the phosphorylation of ACC both *in vitro* and *in vivo*. Fasting increases but refeeding decreases the phosphorylation of AMPK and ACC in CaMKKβ$^{+/+}$ but not CaMKKβ$^{-/-}$ mice. Under *ad libitum* feeding, the increased expression of sterol regulatory element binding protein-1c (SREBP-1c)-mediated lipogenic gene is concurrent with decreased phosphorylation of AMPK-regulated ACC in white adipose tissue (WAT) of

CaMKKβ$^{-/-}$ mice. In line with the inhibitory role of CaMKKβ in lipid synthesis and storage, CaMKKβ$^{-/-}$ mice exhibit increased body weight, adiposity, and adipocyte hypertrophy, although their appetite is comparable with the CaMKKβ$^{+/+}$ littermates. Additionally, metformin, an AMPK activator, does not increase the phosphorylation of AMPK and ACC in WAT of CaMKKβ$^{-/-}$ mice. Thus, the CaMKKβ/AMPK signaling is an important molecular event in physiological and pharmacological (e.g., metformin) regulation of adiposity.

Table of Contents

List of Figures

List of Abbreviations

ACC: acetyl-CoA carboxylase

AICAR: 5'-aminoimidazole-4-carboxamide ribonucleoside

AMPK: AMP-activated protein kinase

ATGL: adipose triglyceride lipase

BMR: basal metabolic rate

CaMKI: Ca^{2+}/calmodulin-dependent protein kinase I

CaMKIV: Ca^{2+}/ calmodulin-dependent protein kinase IV

CaMKK: Ca^{2+}/calmodulin-dependent protein kinase kinase

DMEM: Dulbecco's modified eagle medium

FAS: fatty acid synthase

GTT: glucose tolerance test

HDL: high-density lipoprotein

HMG-CoA: hydroxymethylglutaryl-CoA

HSL: hormone-sensitive lipase

ITT: insulin tolerance test

LDL: low-density lipoprotein

LPL: lipoprotein lipase

MAGL: monoacylglycerol lipase

MEF: mutine embryonic fibroblasts

NPY: neuropeptide Y

PKA: cAMP-dependent protein kinase

PKI: PKA inhibitor

SCD1: stearoyl-CoA desaturase 1

SREBP: sterol regulatory element binding protein

VLDL: very low-density lipoprotein

WAT: white adipose tissue

Chapter 1

Introduction

1.1. Lipid metabolism and adipose tissue

Lipids are important for many biological functions such as energy storage, membrane structure and cell signaling. Adipose tissue is the major organ for storage of lipids in the form of triglycerides, both from circulation and de novo synthesis (lipogenesis). Lipoprotein lipase (LPL), synthesized by adipocytes, can hydrolyze triglyceride-rich lipoproteins such as chylomicrons and very-low-density lipoproteins (VLDLs) recruited from the blood to release free fatty acids. Fatty acids are then transported into adipocytes and re-esterified with glycerol phosphate to form triglycerides, which are then stored in lipid droplets.

The first step of lipogenesis in adipocytes is the biosynthesis of fatty acids, which are the primary components of both triglycerides and phospholipids. Fatty acid synthesis starts from carboxylation of acetyl-CoA to produce malonyl-CoA, an irreversible process catalyzed by acetyl-CoA carboxylase (ACC1/ACC2) (1). The long carbon chains of fatty acids are assembled in a repeated extending process, which is catalyzed by fatty acid synthase (FAS) (1). Other enzymes involved in the lipid synthesis process include acetyl-CoA synthetase, stearoyl-CoA desaturase 1 (SCD1), and glycerol-3-phosphate acyltransferase (2). Nevertheless, ACC1/ACC2 is the rate-limiting enzyme for lipid synthesis.

Adipocytes also release fatty acids into the circulation by breaking down triglycerides, which are used by most organs for fuel when glucose is limited. Triglycerides are hydrolyzed (lipolysis) into fatty acids and glycerol, then exported into the blood. Lipolysis involves several enzymes, including adipose triglyceride lipase (ATGL), hormone-sensitive lipase (HSL), and monoacylglycerol lipase (MAGL) (3-5). ATGL initiates lipolysis by cleaving the first fatty acid from triglycerides, and then HSL and MAGL act on diacyglycerol and monoacylglycerol, respectively, releasing two additional fatty acids and one glycerol molecule (4).

Adipocytes can also modulate lipid mobilization by altering fatty acid oxidation, which is also regulated by ACC2. Malonyl-CoA, formed by ACC2, inhibits carnitine acyltransferase I, which catalyses the entry of fatty acids into mitochondria and constitutes the rate-limiting enzyme of fatty acid oxidation. Enhancement of fatty acid oxidation in white adipose tissue (WAT) has been proposed to reduce adiposity. Mice with ACC2 knockout show increased fatty acid oxidation and decreased fat accumulation as compared with wild-type mice (6). Therefore, the balance among lipogenesis, lypolysis, and fatty acid oxidation in adipocytes is critical for whole-body energy homeostasis. Fig. 1-1 illustrates the key enzymes involved in adipocyte lipid metabolism.

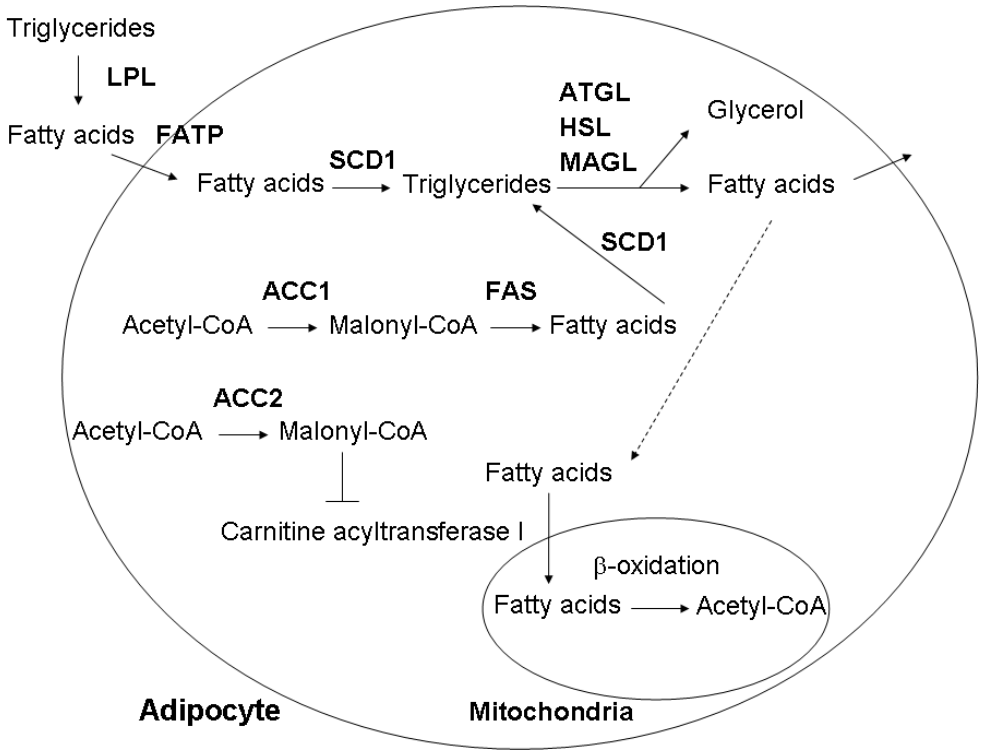

Fig. 1-1. Lipid metatabolism in adipocytes. Key enzymes involved in lipid uptake, lipogenesis, lypolysis, and fatty acid oxidation in adipocytes.

1.2. Regulation of fatty acid synthesis and oxidation by ACC1/ACC2

ACC1/ACC2 catalyzes the rate-limiting step of fatty acid synthesis by converting acetyl-CoA to malonyl-CoA. ACC has two isoforms of different molecular weight: 265 kDa (ACC1 or ACCα) and 280 kDa (ACC2 or ACCβ). Both ACC1 and ACC2 have three functional sites: the ATP binding site, the carboxylation site (biotin binding site) and the acyl-CoA binding site. The major difference between ACC1 and ACC2 is the extended N terminus of ACC2, which directs ACC2 to the mitochondrial membrane (7). ACC1, which lacks this targeting sequence, is localized in the cytosol (7) and is predominately expressed in lipogenic tissues, such

as WAT and mammary glands (8-10). ACC2 is the major form in oxidative tissues, such as heart and skeletal muscle, and governs the transfer of fatty acyl-CoA to the mitochondria for fatty acid oxidation through its regulation of malonyl-CoA (7, 11, 12). Both isoforms are expressed in the liver where both fatty acid synthesis and oxidation are important (9, 11, 12). ACC1 is the predominant form in WAT, but ACC2 is also expressed, which suggests that it plays a role in regulating fatty acid oxidation in WAT (6). Malonyl-CoA formed in the cytosol by ACC1 is used for fatty acid synthesis and elongation, thus leading to triglyceride formation, whereas malonyl-CoA formed at the mitochondrial surface by ACC2 acts primarily in the regulation of mitochondrial fatty acid oxidation (13).

1.2.1 Regulation of ACC1/ACC2 by reversible phosphorylation

ACC1/ACC2 activity is mainly regulated by reversible phosphorylation (14). Phosphorylation of ACC1/ACC2 inactivates it, whereas dephosphorylation of ACC1/ACC2 activates it. ACC1 has eight phosphorylation sites, at S23, 25, 29, 77, 79, 96, 1200, and 1215 (14). Among the identified protein kinases, only cAMP-dependent protein kinase A (PKA) and AMP-activated protein kinase (AMPK) can phosphorylate and inactivate ACC1 *in vitro* (15-18). PKA phosphorylates ACC1 at S77 and S1200, whereas AMPK phosphorylates ACC1 at S79, S1200 and S1215. S77 and S1200 are critical sites for inactivation of ACC1 by PKA, and S79 is a critical site for inactivation by AMPK (15, 19). However, phosphorylation of ACC1

S79 by AMPK is probably the most critical site involved in the inhibition of ACC1 activity (20-22).

Unlike knowledge of phosphorylation sites of ACC1, that of the number and identity of sites in ACC2 is unclear. *In vitro*, PKA (23-25) and AMPK (23, 24) have been shown to phosphorylate ACC2. AMPK phosphorylates ACC2 at S212, which is homologous to S79 of ACC1 in mice. Furthermore, phosphorylation of ACC2 by AMPK, rather than PKA, is more significant for regulation of ACC2 activity and hence fatty acid oxidation in skeletal muscle (24). Although AMPK and PKA potentially phosphorylate and regulate ACC2 activity, knowledge of protein kinases that phosphorylate ACC2 responding to different stimuli is unclear.

1.2.2 Regulation of ACC1/ACC2 by transcriptional regulation

ACC1/ACC2 is also regulated at the transcriptional level. ACC1 and ACC2 gene expression is induced in response to various factors including glucose, insulin, thyroid hormone, catabolic hormones and leptin (14, 26, 27). Sterol regulatory element binding protein 1c (SREBP-1c) is the major transcriptional regulator of ACC1/ACC2 expression responding to hormonal and nutrient signals (28). Other transcription factors that contribute to the control of ACC1/ACC2 expression include carbohydrate response element binding protein (ChREBP), liver X receptor, retinoid X receptor, peroxisome proliferator activated receptors (PPARs), forkhead box O (FOXO) and PPARγ co-activator (PGC) isoforms (29, 30). However, in adipocytes,

the expression of lipogenic enzymes including ACC1/ACC2, FAS, SCD1, LPL are mainly regulated by SREBP-1c (31-33).

1.3. AMPK is an energy sensor and a key regulator of ACC1/ACC2

AMPK, an energy-sensing kinase, is a critical signaling molecule for the regulation of multiple metabolic processes (34, 35). AMPK is activated in response to ATP depletion or an increase in the ratio of AMP to ATP within the cell. Activated AMPK upregulates catabolic pathways and downregulates anabolic pathways to promote ATP generation in peripheral tissues (36-41). Furthermore, orexigenic and anorexigenic signals regulate hypothalamic AMPK, which, in turn, regulates food intake (42-46). AMPK plays a role in the regulation of several aspects of metabolism, including fatty acid synthesis, fatty acid oxidation, lipolysis, glucose transport, gluconeogenesis, and glycolysis in the periphery. The direct downstream targets of AMPK include ACC1/ACC2, FAS, mammalian target of rapamycin, glycerol phosphate acyltransferase, and 3-hydroxy-3-methyl-CoA reductase, which are key regulators of fatty acid, protein, glycerolipid, and cholesterol synthesis, respectively (47). Hardie et al. reviewed all the targets for AMPK in different biosynthetic and catabolic pathways (Fig. 1-2).

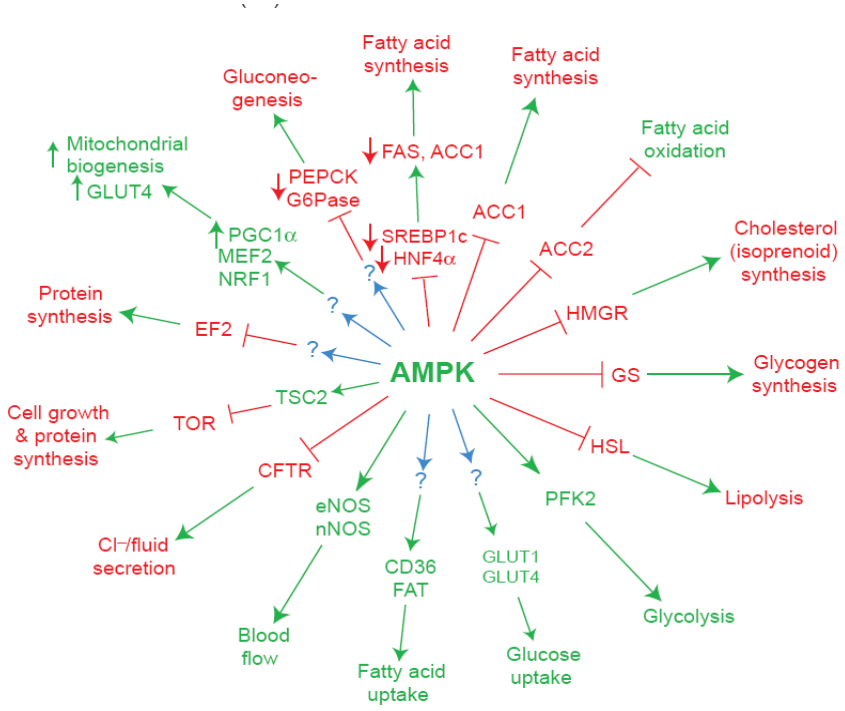

Fig. 1-2. Targets for AMPK. Target proteins and processes activated by AMPK are in green and those inhibited by AMPK are in red. When the effect is caused by a change in gene expression, an upward-pointing green arrow next to the protein indicates an increase in expression, and a downward-pointing red arrow indicates a decrease. CD36/FAT, CD36/fatty acid translocase; CFTR, cystic fibrosis transmembrane regulator; EF2, elongation factor-2; eNOS/nNOS. endothelial/neuronal isoforms of nitric oxide synthase; G6Pase, glucose-6-phosphatase; GLUT1/4, glucose transporters; GS, glycogen synthase; HMGR, 3-hydroxy-3-methyl-CoA reductase; HSL, hormone-sensitive lipase; MEF2, myocyte-specific enhancer factor-2; NRF1, nuclear respiratory factor-1; PEPCK, phosphoenolpyruvate carboxykinase; PGC1α, peroxisome proliferator-activated receptor-γ co-activator-1α; TOR, mammalian target of rapamycin. (Adapted from Hardie 2004) (48)

One of the first proteins identified as a target of AMPK was ACC1 (22). The phosphorylation and thus inhibition of ACC1 by AMPK has been shown both *in vivo* and *in vitro*. In adipocytes, the effect of AMPK activation on ACC1 phosphorylation and activity was shown by with 5-aminoimidazole-4-carboxamide 1-ribofuranoside (AICAR) activation (49) or expression of constitutively active

AMPK (50). AMPK also inhibits ACC2 activity, so activation of AMPK in adipocytes leads to decreased lipogenesis and increased fatty acid oxidation (51, 52). AMPK $\alpha 2^{-/-}$ mice fed a high-fat diet show increased adipose mass due to adipocyte hypertrophy as compared with control mice (53). AMPK seems to be the major physiological ACC1/ACC2 kinase; however, the role of PKA inactivating ACC1/ACC2 should not be ignored. Recently, Li et al. showed that AMPK directly phosphorylates SREBP-1c and suppresses its cleavage and nuclear translocation, thereby blocking lipogenic gene transcription (54). Therefore, AMPK regulates ACC1/ACC2 activity and transcription.

1.4. Regulation of AMPK by CaMKKβ

AMPK exists as a heterotrimeric enzyme consisting of a catalytic subunit (α) and two regulatory subunits (β and γ) that play important roles in determining the substrate specificity and maintaining protein stability. Several isoforms have been identified for each subunit ($\alpha 1$, $\alpha 2$, $\beta 1$, $\beta 2$, γ 1, γ 2, γ 3) (55). These combinations confer different properties to the AMPK complexes (56) and relative tissue specificity (57). For the catalytic α subunit, the $\alpha 1$ isoform is widely distributed, whereas the $\alpha 2$ isoform is highly expressed in muscle and liver but also found in adipocytes (58, 59).

AMPK activation requires the phosphorylation of T172 in the activation loop of the catalytic α subunit by an upstream AMPK kinase (AMPKK). Two major AMPKKs have been characterized. LKB1 is a Ser/Thr kinase that can

phosphorylate and activate AMPK activity (60, 61). Previous studies have indentified LKB1 in muscle, liver, and WAT (50, 62-64). In addition to LKB1, Ca^{2+}/calmodulin-dependent protein kinase kinase β (CaMKKβ) can phosphorylate and activate AMPK in the presence of increased calcium concentration (65). Expressed abundantly in the brain (66), CaMKKβ controls food intake by regulating hypothalamic AMPK, thus leading to the production of the orexigenic hormone neuropeptide Y (NPY) (67). Although many studies show that LKB1 acts as an AMPKK in the periphery (50, 62, 68, 69), Gormand et al. showed that CaMKKβ may be involved in AMPK activation in cultured adipocytes (70). However, we lack evidence of the role of CaMKKβ in regulating AMPK and its downstream functions in adipose tissue *in vivo*. Therefore, whether peripheral CaMKKβ regulates AMPK pathways in response to hormonal and nutrient signals remains unknown.

CaMKK has 2 isoforms: a 505 amino acid α isoform and a slightly larger β isoform composed of 587 amino acids. CaMKKβ is expressed primarily in the brain, but CaMKKα is also expressed in the thymus and spleen (71). CaMKK resides in the cytosol and nucleus of the cell, where it can respond to both cytosolic and nuclear changes in Ca^{2+} concentration and act on its two known substrates, Ca^{2+}/calmodulin-dependent protein kinase I (CaMKI) and Ca^{2+}/ calmodulin-dependent protein kinase IV (CaMKIV). CaMKK also mediates cell death as a substrate for death-associated protein kinase (DAPK), thus extending its

known cellular role (72). Recently, CaMKKβ was shown to function as physiologically relevant AMPKK in cells (73-75). In contrast to activation directed by AMP/LKB1, the CaMKKβ-dependent activation of AMPK operates independently of AMP. The role of CaMKKβ in AMPK regulation in adipocytes remains unclear.

1.5. Glucagon regulation of lipogenesis

Fatty acid synthesis in adipocytes is regulated by several hormones, including glucagon, insulin, epinephrine, norepinephrine, adipokines, and thyroid hormones, and the elicited signaling pathways coordinate whole-body lipid metabolism. Insulin and glucagon are two counter-regulatory hormones that regulate lipid metabolism responding to nutrient status. Insulin promotes lipid storage through upregulating fatty acid synthesis by enhancing ACC1/ACC2 activity, whereas glucagon decreases fatty acid synthesis by inhibiting ACC1/ACC2 activity (76-78).

Glucagon was originally demonstrated to increase the use of stored carbohydrates, opposite to the effect of insulin (79). The catabolic action of glucagon promoting the breakdown of glycogen to glucose in concert with the anabolic action of insulin promoting glucose storage as glycogen allows these two hormones to tightly regulate blood glucose levels. Upon post-absorption, fasting, or starvation, the increased glucagon secretion enhances the blood glucose level by promoting glycogenolysis and gluconeogenesis in the liver (80). However, a growing body of data demonstrates that the physiologic role of glucagon extends

beyond glucose homeostasis (81). In addition to expression in liver, glucagon receptors are expressed in the heart, lymphoblasts, brain, retina, adrenal gland, gastrointestinal tract, and adipocytes (82). The action of glucagon on adipocytes is particularly intriguing because of the increasing prevalence of adiposity and its close association with metabolic diseases (81).

Glucagon regulates lipid metabolism in adipocytes by modulating the activity of ACC1/ACC2 (76, 78). Low dietary carbohydrate level and thus low blood glucose level induces the release of glucagon, thus resulting in increased phosphorylation and inactivation of ACC1/ACC2. Glucagon is a peptide hormone synthesized and secreted from α cells of the islets of Langerhans in the pancreas. Glucagon signals by binding to glucagon receptors on the cell surface. The glucagon receptor is a member of the G-protein-coupled family of receptors, and at least two classes of G proteins, Gsα and Gq, are involved in the signal transduction of the glucagon receptor (83). The activation of Gsα leads to activation of adenylate cyclase, increased intracellular cAMP levels, and subsequent activation of PKA, which induces downstream signaling pathways to regulate glucose and lipid metabolism. The activation of Gq leads to the activation of phospholipase C, production of inositol 1,4,5-triphosphate, and subsequent increase of intracellular calcium ($[Ca^{2+}]_i$), which is cAMP independent (84-86). Fig. 1-3 illustrates the glucagon signaling pathways involving both Gsα and Gq.

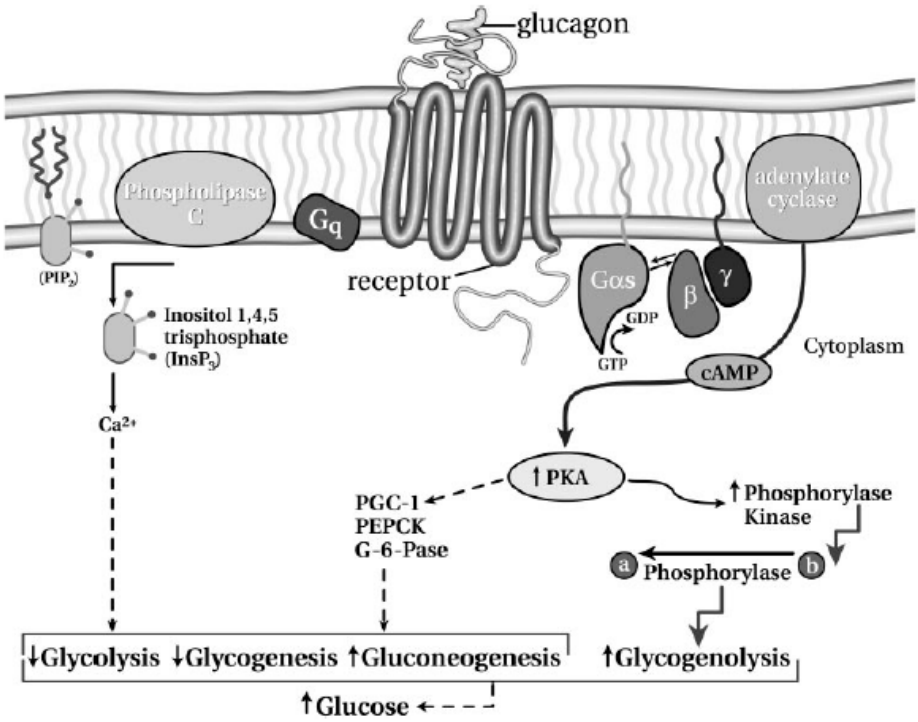

Fig. 1-3. Glucagon-signaling pathway. PIP2, phosphatidylinositol 4,5-biphosphate; PGC-1, peroxisome proliferator-activated receptor-γ coactivator-1; PEPCK, phospho*enol*pyruvate carboxykinase; G-6-Pase, glucose-6-phosphatase. (Adapted from Jiang 2003) (83)

Glucagon-mediated inhibition of ACC1 in isolated hepatocytes and adipocytes may be through increased phosphorylation of ACC1 by PKA (87, 88). However, other studies have shown ACC1 phosphorylation in glucagon-treated hepatocytes (22) or adrenaline-treated adipocytes (21), likely because of modulation by AMPK. Therefore, the molecular basis of glucagon-regulated fatty acid synthesis remains unclear. The observation that S77 remains dephosphorylated *in vivo* suggested that AMPK is the major kinase that could physiologically inactivate ACC1 (89). Chapter 2 examines the role of CaMKKβ/AMPK in glucagon-regulated ACC1/ACC2 activity.

1.6. SREBP-1c regulation of lipogenesis

Synthesis of both fatty acid and cholesterol is controlled by a common family of transcription factors, SREBPs. SREBPs are synthesized as inactive precursors bound to the endoplasmic reticulum (ER) membranes. The precursor of SREBPs migrates from the ER to the Golgi and undergoes sequential proteolytic processing to release the transcriptionally active N-terminal domain into the nucleus and are thus designated nSREBPs. Once nSREBPs translocate into the nucleus, they bind to functional sterol regulator elements (SREs) present in promoters/enhancers of SREBPs and their target genes to activate the transcription of SREBPs and SREBP-responsive genes that control the synthesis of fatty acids and cholesterol (2, 90).

Three members of the SREBP family have been described in several mammalian species. SREBP-1a and 1c are produced from a single gene (*SREBF-1*) (91) and SREBP-2 from a separate gene (*SREBF-2*) (92). SREBP-1a and 1c transcripts are produced through the use of alternative transcription start sites and differ in their first exon (exon 1a and exon 1c), but the other exons are common to both isoforms. SREBP-1a is a more potent transcriptional activator than SREBP-1c because of its longer NH_2-terminal transactivation domain (93). However, SREBP-1c is the predominant isoform expressed in most tissues of mice and humans, with especially high levels in the liver, WAT, skeletal muscle, adrenal gland and brain (94). In contrast, SREBP-1a is highly expressed in cell lines and tissues with high

propensity for cell proliferation, such as spleen and intestine (94). Fig. 1-4 illustrates the biosynthetic pathways used to generate cholesterol and fatty acids that are regulated by SREBP-2 and -1c (2). SREBP-1c is key transcription factor associated with lipogenesis and adipocyte development in WAT (94, 95). The expression of several lipogenic enzymes, including ACC1, ACC2, FAS, SCD1, and LPL, are mainly regulated by SREBP-1c in adipocytes (31-33, 96, 97).

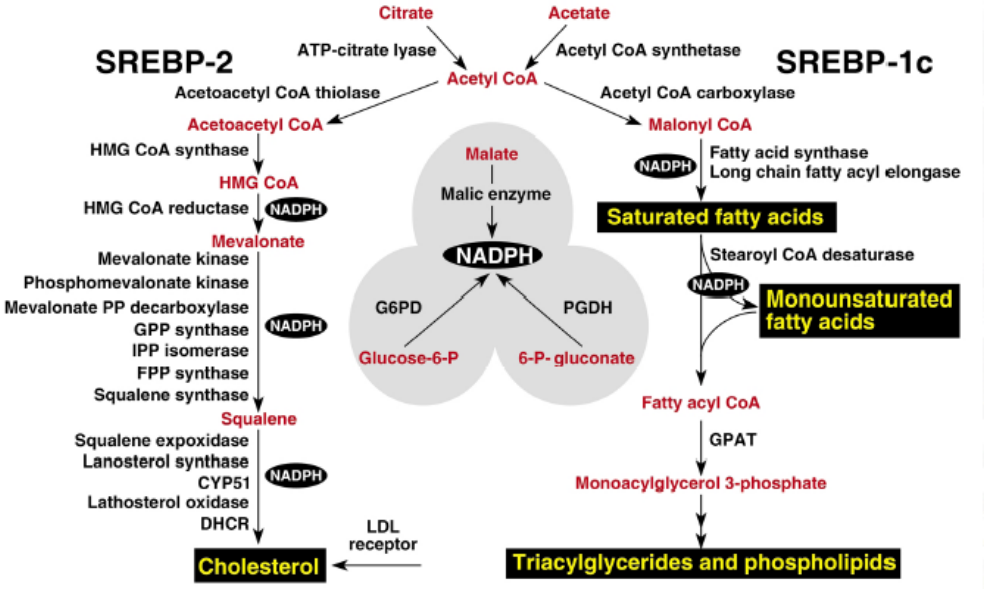

Fig. 1-4. Genes regulated by SREBPs. The diagram illustrates the major metabolic intermediates for synthesis of cholesterol, fatty acids, and triglycerides. *In vivo*, SREBP-2 preferentially activates genes of cholesterol metabolism, whereas SREBP-1c preferentially activates genes of fatty acid and triglyceride metabolism. DHCR, 7-dehydrocholesterol reductase; FPP, farnesyl diphosphate; GPP, geranylgeranyl pyrophosphate synthase; CYP51, lanosterol 14α-demethylase; G6PD, glucose-6-phosphate dehydrogenase; PGDH, 6-phosphogluconate dehydrogenase; GPAT, glycerol-3-phosphate acyltransferase. (Adapted from Horton 2002) (2)

In mouse adipose tissue, SREBP-1c mRNA expression is greatly reduced by fasting by an insulin-dependent mechanism (32). Subsequent experiments in

isolated adipocytes (32) and hepatocytes (96) demonstrated that the transcription of SREBP-1c is induced by insulin. This induction of SREBP-1c transcription leads to a parallel increase in expression of both the ER membrane-bound precursor and the nuclear form of the active transcription factor (98). The effects of insulin on SREBP-1c transcription are opposed by glucagon via cAMP (97). SREBP-1c transcription can be induced by activation of liver X receptor (LXR)α, a nuclear hormone receptor (99). However, the transcription factor interferon regulatory factor 4 (IRF4) can inhibit the transcription of SREBP-1c (100). Moreover, SREBP-1c is negatively regulated by AMPK (101-103). AMPK directly phosphorylates SREBP-1c to suppress its cleavage and nuclear translocation, thereby blocking lipogenic gene transcription (54). Thus, CaMKKβ/AMPK signaling may also regulate lipogenic gene expression through SREBP-1c. Chapter 3 describes the role of CaMKKβ/AMPK in the regulation of lipogenic gene expression.

Chapter 2

Glucagon regulates ACC1/ACC2 activity through CaMKKβ/AMPK pathway in adipocytes

2.1 Abstract

Glucagon is important in regulating lipid metabolism, in part through its inhibition of fatty acid synthesis in adipocytes. Given that ACC1 is the rate-limiting enzyme for fatty acid synthesis, the proposed mechanism is glucagon activating PKA, which in turn phosphorylates ACC1 at S77 and S1200, and thereby attenuates the lipogenic activity of ACC1. Because AMPK also inhibits FA synthesis by phosphorylating ACC1 S79, I examined the involvement of AMPK in the glucagon-elicited signaling in adipocytes. In this chapter, I report that glucagon induces ACC1 S79 and ACC2 S212 phosphorylation through CaMKKβ/AMPK pathway *in vitro* and *in vivo*. LC/MS/MS analysis revealed that ACC1 was phosphorylated only at S79 in glucagon-treated adipocytes. Experiments with pharmacological inhibition or siRNA knockdown of AMPK or PKA revealed that glucagon regulated ACC1 and ACC2 activity through AMPK, not PKA. Furthermore, AMPKα2$^{-/-}$ and CaMKKβ$^{-/-}$ mice treated with glucagon showed no phosphorylation of ACC1 S79 or ACC2 S212 in WAT. Therefore, CaMKKβ/AMPK is crucial in regulating the glucagon-elicited lipid metabolism in adipocytes.

2.2 Introduction

Glucagon is a peptide hormone synthesized in and secreted from α cells of the islets of Langerhans of the pancreas. With fasting or starvation, glucagon is released into blood plasma and enhances the blood glucose level by increasing glycogenolysis and gluconeogenesis in the liver. Glucagon also plays an important role in regulating fatty acid metabolism largely by modulating the activity of ACC1, the rate-limiting enzyme in fatty acid synthesis. Previous studies have shown that these actions are mediated by glucagon receptors belonging to the G-protein-coupled receptor family. Stimulation of the glucagon receptor results in increased cellular cAMP level, which in turn activates PKA. However, the molecular basis of glucagon-regulated fatty acid synthesis by PKA remains unclear.

ACC has two major isoforma, ACC1 and ACC2. ACC1 is the predominant isoform expressed in lipogenic tissues, such as WAT and mammary glands, and is the major form regulating fatty acid synthesis, whereas ACC2 is preferentially expressed in skeletal muscle and mainly regulates fatty acid oxidation. Although ACC1 is the predominant form expressed in WAT, ACC2 is also expressed in WAT, so it may play a role in regulating fatty acid oxidation in WAT as well (6). ACC1/ACC2 activity can be regulated at both transcriptional and post-translational levels. Reversible phosphorylation represents a major post-translational modification of ACC1/ACC2 by stimuli such as glucagon. Among the several identified protein kinases, only PKA and AMPK inactivate ACC through phosphorylation *in vitro*. Specifically,

phosphorylation at S79 is required for the inhibition of ACC1 activity by AMPK, whereas S1200 and S77 are necessary for inactivation of ACC1 by PKA.

AMPK is widely recognized as a cellular energy gauge by governing multiple metabolic processes. Various stimuli can induce phosphorylation of AMPK by LKB1 or CaMKKβ at T172 in the activation loop of the α subunit, thus leading to its activation. The key role of AMPK in lipid metabolism is largely mediated by phosphorylation of ACC1 at S79 and ACC2 at S212, which results in inhibition of ACC1 and ACC2 activity. Given that adipocyte is the major tissue where lipid is metabolized and the lack of information about glucagon-activated AMPKK, I examined the elicited pathways and functional consequences in adipocytes responding to glucagon.

2.3 Materials and Methods

2.3.1 Antibodies and reagents

Antibodies against phospho-AMPKα T172, AMPKα, phospho-ACC1 S79/ACC2 S212, phospho-CREB S133, PKA and α-tubulin, GST-AMPKα, GST-CaMKKβ, and PKA C-α were from Cell Signaling. Anti-CaMKK was from BD Biosciences Pharmingen. Anti-ACC, anti-phospho-CaMKI T177 and anti-β-actin were from Santa Cruz Biotechnology. Compound C, bovine brain calmodulin (CaM), and myristoylated-PKA inhibitor amide 14-22 (PKI) were from Calbiochem. Glucagon, STO-609, 5-aminoimidazole-4-carboxamide

1-ribofuranoside (AICAR), Fura-2-AM, EGTA, and ATP were from Sigma. The siRNA targeting AMPK, PKA, CaMKKβ, and LKB1, and scramble RNA were from QIAGEN.

2.3.2 Cell culture and transient transfection

Murine 3T3-L1 preadipocytes were cultured, maintained, and differentiated as described (104). Briefly, cells were plated and grown for 2 days post-confluence in DMEM supplemented with 10% calf serum. Differentiation was then induced by changing the medium to DMEM supplemented with 10% fetal bovine serum (FBS), 0.5 mM 3-isobutyl-1-methylxanthine, 1 μM dexamethasone, and 1.7 μM insulin. After 48 hr, the differentiation medium was replaced with a maintenance medium containing DMEM supplemented with 10% FBS. The maintenance medium was changed every 48 hr. The induction lasted for 8 days until the cells were used for experiments. Wild-type and CaMKKβ$^{-/-}$ mutine embryonic fibroblasts (MEFs) were isolated from the wild-type C57BL/6 and CaMKKβ$^{-/-}$ mouse embryos (E13) and cultured *in vitro* by a standard protocol (105). LKB1$^{-/-}$ and AMPK$^{-/-}$ MEFs were gifts from Dr. Reuben Shaw (Salk Institute). Differentiation of MEFs was induced as described (106). Transient transfection involved use of Lipofectamine RNAiMAX (Invitrogen). 3T3-L1 adipocytes were transfected with scramble, AMPK, PKA, CaMKKβ or LKB1 siRNA (10 nM) in Opti-MEM (Gibco). Four hours after transfection, the medium was changed to fresh DMEM supplemented with 10% FBS.

At 72-hr post-transfection, cells were exposed to 100 nM glucagon for 2 hr. For inhibition experiments, the cells were pretreated with 20 μM compound C, 10 μM PKI, or 5.3 μM STO-609 for 30 min before glucagon exposure. For the activation of AMPK with AICAR, cells were treated with 1 mM AICAR for 30 min.

2.3.3 Western blot analysis

After treatment, cells were harvested and lysed. After protein quantification, an equal amount of total protein was resolved by 8% SDS-PAGE and then transferred to a PVDF membrane. The samples were immunoblotted with primary antibodies as indicated, and then horseradish peroxidase-conjugated secondary antibodies. The recognized bands were visualized by an enhanced chemiluminescence detection kit (Amersham Biosciences) and quantified by use of ImageJ.

2.3.4 Nano-liquid chromatography tandem mass spectrometry (Nano-LC/MS/MS)

ACC1 was immunoprecipitated from 4 mg glucagon-treated 3T3-L1 adipocytes lysates by 8 μg of anti-ACC1 antibody. The phosphorylation of immunoprecipitated ACC1 was detected by Nano-LC/MS/MS analysis, which involved the Q-TOF Premier mass spectrometer, nano-Acquity ultra-performance liquid chromatography (UPLC), with a BEH130 C_{18} analytical column (Waters Corp.). The immunoprecipitated ACC1 was first trypsin-treated and then purified with use of titanium dioxide (TiO_2)-coated magnetic beads provided with the Phos-Trap

phosphopeptide enrichment kit (PN# PRT302001KT, Perkin Elmer). The bound phosphopeptides were collected and lyophilized. The freeze-dried pellet was dissolved in 0.1% trifluoroacetic acid for Nano-LC/MS/MS. The phosphorylation sites within the ACC1 phosphopeptide were determined by a characteristic neutral loss of the phosphate group during collision-induced dissociation.

2.3.5 Intracellular calcium imaging

3T3-L1 adipocytes were cultured on coverslips to 100% confluence, loaded with the ratiometric Ca^{2+} indicator Fura-2/acetoxymethyl ester (Invitrogen, 2 μM) in Tyrode's solution containing 0.05% Pluronic F-127 for 30 min at 37°C, and mounted on the stage of a Nikon TE300 inverted fluorescence microscope. Washed cells were illuminated alternately at 340 and 380 nm, and the emitted light was collected with a 40x objective (Nikon S-Fluor, NA 0.9) through a 490-530 nm bandpass filter. Images were captured every 2 min by use of a cooled CCD digital camera (Hamamatsu Orca-100) and analyzed by use of MetaFluor software (Molecular Devices). Background-corrected 340/380 nm ratios from defined regions of cells were used to monitor local free Ca^{2+} concentration over time with calibration parameters determined at the end of each experiment.

2.3.6 *In vitro* kinase assay

GST-AMPKα1 (44 nM) or PKA (95 nM) were incubated with synthesized 1 mM ACC1 peptide (HMRSSMSGLHLVKQG) or SAMS peptide

(HMRSAMSGLHLVKRR) in 25 μl HEPES buffer (50 mM, pH 7.4) containing 5 mM $MgCl_2$, 0.2 mM ATP, and 0.2 mM AMP. The kinase activity of AMPK or PKA, in the presence of GST-CaMKKβ (46 nM) and/or Ca^{2+} (2 mM)/CaM (2 μM), was determined by ACC1 or SAMS peptide phosphorylation. The phosphorylation site of ACC1 or SAMS peptide was determined by Nano-LC/MS/MS. The phosphorylation level changes in ACC1 and SAMS peptides were quantified by the selected ion monitoring mode of LC.

2.3.7 Animal experiments

The animal experimental protocols were approved by the UCR institutional Animal Care and Use Committee. Twelve-week-old male C57BL/6, CaMKKβ$^{+/+}$, CaMKKβ$^{-/-}$, AMPKα2$^{+/+}$ or AMPKα2$^{-/-}$ mice were housed with a 12-hr light/12-hr dark cycle with free access to regular chow unless otherwise described. For glucagon experiments, mice were given glucagon (5 μg/kg) or saline as a vehicle control by intraperitoneal injection, for 30 min and 1, 2 and 4 hr. Epididymal fat pads and livers were collected for Western blot analysis.

2.3.8 Statistical analysis

Unless indicated, results are expressed as mean ± SEM from three independent experiments. Experiments comparing two groups were analyzed by Student *t* test. Differences among multiple groups were initially evaluated by ANOVA, then Dunnett or Newman-Keuls post-hoc test with GraphPad Prism 4 for Windows (GraphPad

Software Inc.). Unless otherwise indicated, *p<0.05 was considered statistically significant.

2.4 Results

AMPK mediates glucagon-induced ACC1/ACC2 phosphorylation in adipocytes

To explore the glucagon-induced molecular pathways in adipocytes, I initially examined the time- and dose-dependence of glucagon-induced phosphorylation of AMPK, ACC1, and ACC2 in cultured adipocytes. As illustrated in Fig. 2-1A, glucagon treatment of 3T3-L1 and MEF-derived adipocytes increased the phosphorylation of ACC1 at S79 and ACC2 at S212 time and dose dependently, similar to that reported for hepatocytes (22). Concurrently, the phosphorylation of AMPK at T172, the putative target of CaMKKβ, was increased by glucagon treatment. LC/MS/MS analysis was used to determine the possible site(s) of glucagon-induced phosphorylation of ACC1 in 3T3-L1 adipocytes. Although previous studies suggested that PKA phosphorylates ACC1 at S77 (15, 18), Fig. 2-1B illustrates that glucagon induced the phosphorylation of ACC1 only at S79. A trypsin-digested fragment containing S1200 was not phosphorylated by glucagon (data not shown), although this site is also a presumed PKA phosphorylation site (19).

To provide additional evidence that AMPK, not PKA, mediates glucagon-induced regulation of the two ACC isoforms, AMPK and PKA in 3T3-L1 adipocytes were knocked down by siRNA, and the effects of glucagon were examined.

As shown in Fig. 2-1C, the glucagon-induced phosphorylation of ACC1 and ACC2 was dampened in AMPK siRNA- but not in PKA siRNA-transfected adipocytes, although glucagon activates both AMPK and PKA as revealed by the increased phosphorylation of AMPK and cAMP response element binding (CREB) protein. Similarly, compound C, an AMPK inhibitor, but not myristolylated PKI, a membrane-permeable PKA inhibitor, impaired the phosphorylation of ACC1 and ACC2 (Fig. 2-1D).

CaMKKβ mediates glucagon activation of AMPK

I next studied the ability of glucagon to activate AMPK in wild-type, CaMKKβ$^{-/-}$, LKB1$^{-/-}$, and AMPK$^{-/-}$ MEF-derived adipocytes to determine whether CaMKKβ or LKB1 mediates the glucagon activation of AMPK. As illustrated in Fig. 2-2A, glucagon-induced AMPK, ACC1, and ACC2 phosphorylation was attenuated in both CaMKKβ$^{-/-}$ and AMPK$^{-/-}$ but not LKB1$^{-/-}$ adipocytes. In a second series of experiments, the ability of glucagon to induce AMPK, ACC1 and ACC2 phosphorylation was abolished in 3T3-L1 adipocytes transfected with CaMKKβ siRNA but not LKB1 siRNA (Fig. 2-2B). Further evidence that CaMKKβ mediates glucagon-induced AMPK activation was observed by STO-609, a selective CaMKK inhibitor, attenuating glucagon-induced phosphorylation of AMPK, ACC1, and ACC2 (Fig. 2-2C). Because CaMKKβ is known to be activated by intracellular calcium $[Ca^{2+}]_i$ (107), I determined the effect of glucagon on free $[Ca^{2+}]_i$ in cultured

adipocytes. Imaging of Fura-2-loaded adipocytes revealed that glucagon elevated free $[Ca^{2+}]_i$ after approximately 30 min (Fig. 2-2D). Thus, glucagon increases $[Ca^{2+}]_i$, which in turn activates CaMKKβ in adipocytes.

An *in vitro* kinase assay was then used to investigate whether Ca^{2+}/CaMKKβ can directly activate the AMPK-ACC axis. As illustrated in Fig. 2-3A, purified GST-AMPKα1 in the presence of CaMKKβ could phosphorylate a synthetic ACC1 peptide at the residue corresponding to S79, and the inclusion of Ca^{2+}/CaM greatly enhanced the phosphorylation of this site by AMPK. However, PKA, failed to phosphorylate S79 in the ACC1 peptide in the presence or absence of Ca^{2+}/CaM and CaMKKβ. PKA phosphorylated the ACC1 fragment at the residue corresponding to S77, but this effect was only marginally enhanced by the addition of Ca^{2+}/CaM and CaMKKβ. Similar results were obtained with SAMS peptide, which is derived from ACC1 sequence with Ala substituted at S77 (Fig. 2-3B).

CaMKKβ and AMPK are necessary for glucagon-increased ACC1/ACC2 phosphorylation *in vivo*

To verify that the glucagon-elicited CaMKKβ-AMPK-ACC axis is functional in WAT *in vivo*, glucagon was administered to C57BL/6 mice and caused an increase in the phosphorylation of AMPK, ACC1, and ACC2 in epididymal fat pads that lasted for 2 hr (Fig. 2-4A). The phosphorylation of CaMKI, the canonical downstream target of CaMKK, was also increased. The increased phospohorylation of AMPK,

ACC1, ACC2, and CaMKI was found in the liver of these animals (Fig. 2-5A). Importantly, ablation of AMPKα2 and CaMKKβ in mice abolished the glucagon-induced ACC1 and ACC2 phosphorylation in fat tissue (Fig. 2-4, B and C) and liver (Fig. 2-5, B and C), as compared with littermates. However, glucagon still activated PKA even in the absence of AMPKα2 or CaMKKβ. Therefore, the CaMKKβ/AMPK but not PKA pathway is necessary for glucagon-induced phosphorylation of ACC1 at S79 and ACC2 at S212 in both adipocytes and hepatocytes at the organ level.

To explain why ACC1 is only phosphorylated by AMPK *in vivo*, I performed structure modeling to show the interaction between ACC1 and AMPK, as well as ACC1 and PKA. As shown in Fig. 2-6A, S79 of ACC1 fits with the consensus recognition motif for AMPK, but S77 of ACC1 fits with the consensus recognition motif for PKA. Also, use of Accelrys discovery studio 2.1 to simulate the binding between AMPK and ACC1 or PKA and ACC1 revealed that S79 of ACC1 is close to the catalytic residue D139 of AMPK and S77 of ACC1 is close to the catalytic residue D167 of PKA (Fig. 2-6B and C).

2.5 Discussion

It appears that glucagon increases AMPK and ACC1/ACC2 phosphorylation through CaMKKβ in adipocytes (Fig. 2-2, A-C, and Fig. 2-4, A-C) and liver (Fig. 2-5, A-C). Our results are consistent with previous findings that glucagon administration increased the AMPK phosphorylation but not LKB1 activity in the liver (108).

Mediated by $G\alpha_q$, glucagon increases intracellular [Ca^{2+}] in HEK293 cells (86). Because glucagon increased [Ca^{2+}] in 3T3-L1 adipocytes (Fig. 2-2D), like other [Ca^{2+}] elevating agents, it may activate AMPK through CaMKKβ, independent of LKB1 (73-75, 109, 110). The activation of CaMKKβ/AMPK by glucagon indicates that CaMKKβ/AMPK is one of the major pathways controlling ACC1/ACC2 activity in response to hormonal signals in adipose tissue.

Glucagon and its receptor coupled to $G\alpha_s$ also increases the intracellular level of cAMP. The ensuing activated PKA may phosphorylate and inhibit ACC1 in isolated rat hepatocytes and adipocytes (87, 88). Residues S77 and S1200 seem to be PKA phosphorylation sites, whereas S79 is exclusively phosphorylated by AMPK (15, 18, 19). LC/MS/MS analysis revealed only S79 phosphorylation in glucagon-treated adipocytes (Fig. 2-1B), which suggests that AMPK is the major kinase to regulate ACC1 activity responding to glucagon. Depending on the stimuli, AMPK and PKA can be effector of each other (111-113). However, our results show that glucagon activates AMPK and PKA independently, because knock-down or inhibition of PKA had little effect on glucagon-activated AMPK and vice versa (Fig. 2-1, C and D).

Glucagon-activated PKA triggers several acute effects, including gluconeogenesis and glycogen breakdown in the liver, which is the canonical function of glucagon (83). However, glucagon also inhibits fatty acid synthesis and enhances fatty acid oxidation by regulating ACC1/ACC2 activity, which is mainly controlled by

AMPK (Fig. 2-1). Because PKA is a more ancient protein kinase than AMPK during evolution, PKA may be involved in both glucagon-regulated glucose and lipid metabolism in prokaryotes. In eukaryotes, glucagon-regulated glucose and lipid metabolism are controlled separately by PKA and AMPK, respectively. Thus, glucagon-regulated glucose metabolism may be mediated through a cAMP/PKA pathway, which causes a rapid change of blood glucose level. In contrast, glucagon-regulated lipid metabolism is regulated through a Ca^{2+}/CaMKKβ/AMPK pathway leading to decreased fat accumulation.

Although both AMPK and PKA are activated by glucagon, ACC1 is likely to be a better substrate for AMPK binding. Structural modeling demonstrates that S79 of ACC1 is close to the catalytic residue D139 of AMPK and S77 of ACC is close to the catalytic residue D167 of PKA (Fig. 2-6B). The binding affinity between AMPK and ACC1 or PKA and ACC1 can be examined by competition kinase assay. In this putative experiment, both AMPK and PKA will be mixed with ACC1 peptide in ratios of 1:1, 1:2, or 2:1, and then thephosphorylation of ACC1 peptide will be detected by LC/MS/MS. If ACC1 is a better substrate for AMPK binding, the major phosphorylation site in ACC1 would be S79. Further structural modeling can be performed to show the competition between AMPK and PKA for binding to ACC1. These analyses will be helpful to explain the glucagon-induced AMPK phosphorylation of ACC1, which is not mediated by PKA.

Fig. 2-1

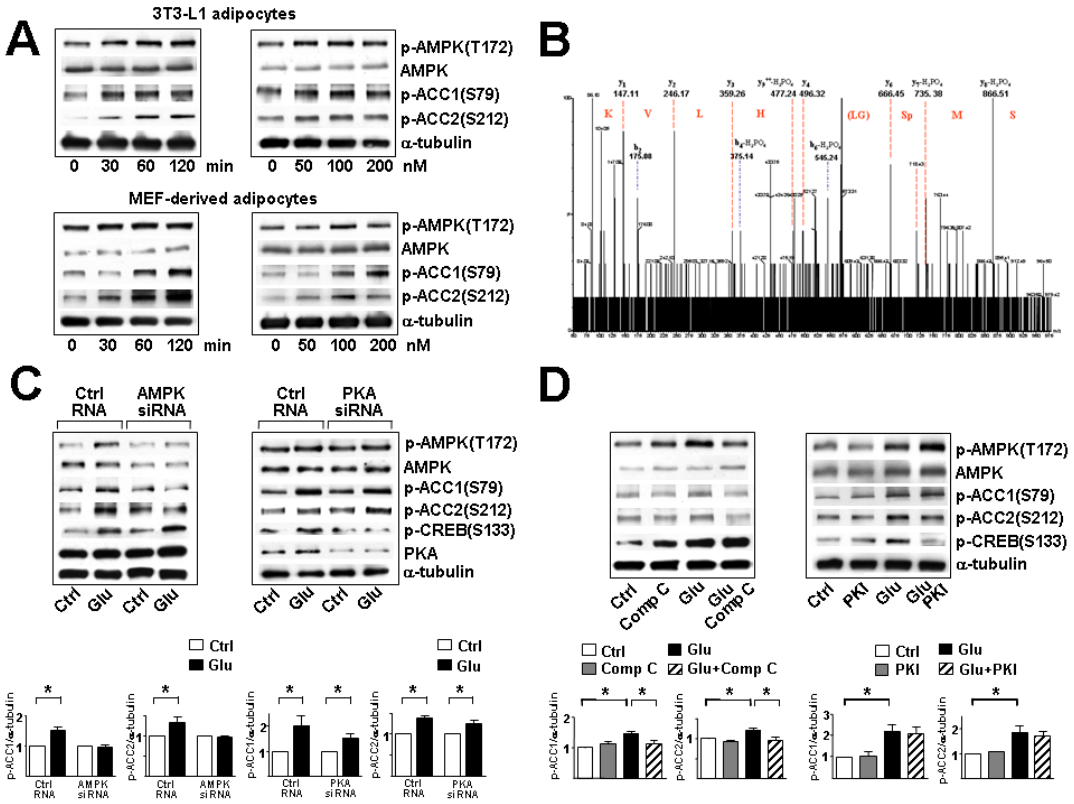

Fig. 2-1. Glucagon-induced ACC1/ACC2 phosphorylation in adipocytes is mediated by AMPK. (**A**) 3T3-L1 and MEF-derived adipocytes were treated with glucagon (100 nM) for the times indicated or various concentrations for 2 hr. (**B**) ACC immunoprecipitated from glucagon-treated 3T3-L1 adipocytes was trypsin digested, and the phosphopeptides were concentrated by use of TiO_2-coated magnetic beads. Nano-LC/MS/MS was performed to map the phosphorylation site(s) within the peptide containing ACC1 S77 and S79. (**C**) 3T3-L1 adipocytes were transfected with AMPK siRNA, PKA siRNA, or control RNA (10 nM). (**D**) 3T3-L1 adipocytes were treated with compound C (20 μM) or myristolylated PKI 14-22 amide (10 μM) for 30 min. Cells in (**C**) and (**D**) were then treated with glucagon (100 nM) for 2 hr. Western blot analysis was performed on cell lysates (**A**, **C**, and **D**) to detect the phospohorylation of AMPK T172, ACC1 S79, ACC2 S212, and CREB S133. The bar graphs represent densitometry analyses of the ratios of phospho-ACC1 S79 or phospho-ACC2 S212 to α-tubulin. Data represent mean ± SEM from 3 independent experiments, with control groups set as 1. *$p < 0.05$ between indicated groups.

Fig. 2-2

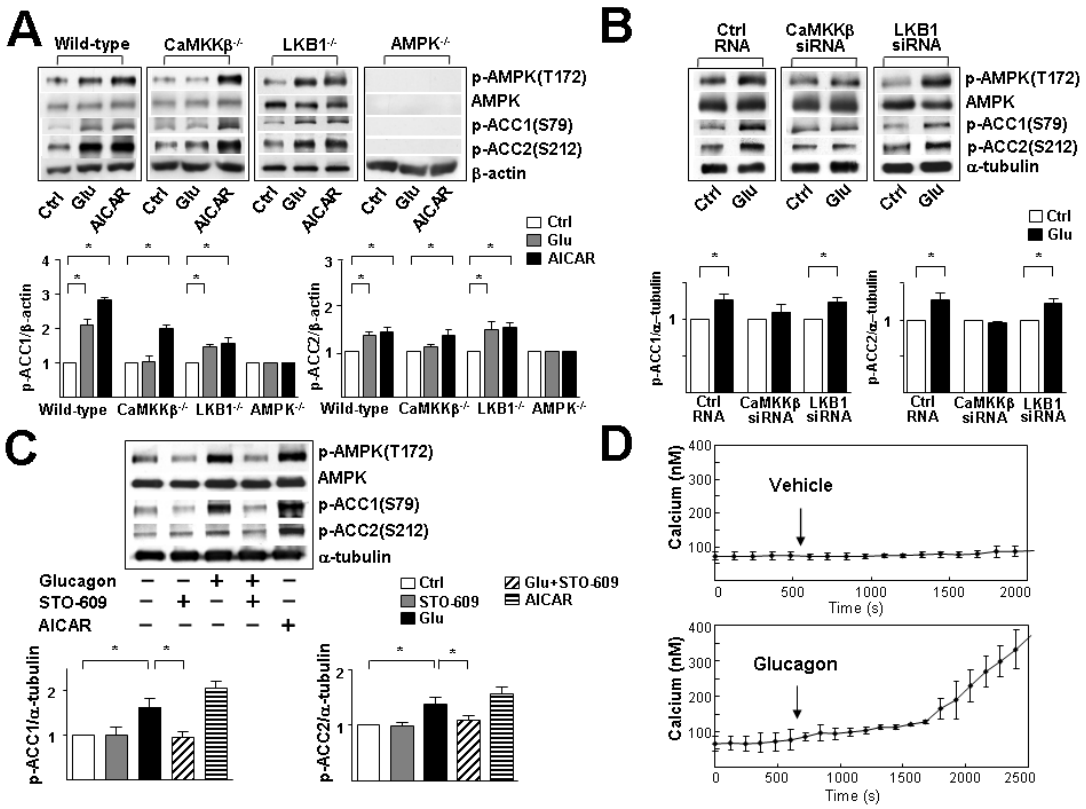

Fig. 2-2. CaMKKβ phosphorylates AMPK in response to glucagon. (**A**) Wild-type, CaMKKβ$^{-/-}$, LKB1$^{-/-}$, and AMPK$^{-/-}$ MEF-derived adipocytes were treated with 100 nM glucagon for 2 hr. The positive control was cells treated with AICAR (1 mM) for 30 min. (**B**) 3T3-L1 adipocytes were transfected with scramble, CaMKKβ, or LKB1 siRNA (10 nM) before glucagon treatment. (**C**) 3T3-L1 adipocytes were treated with STO-609 (5.3 μM) for 30 min before glucagon treatment for 2 hr. In parallel controls, cells were stimulated with AICAR for 30 min. Western blot analysis involved antibodies against phospho-AMPK T172, AMPK, phospho-ACC1 S79, phospho-ACC2 S212, β-actin, and α-tubulin. The bar graphs represent densitometry analyses of the ratios of phospho-ACC1 S79 or phospho-ACC2 S212 to β-actin or α-tubulin. Data represent mean ± SEM from three independent experiments, with control groups set as 1. *$p < 0.05$ between indicated groups. (**D**) Glucagon (100 nM) was added to 3T3-L1 adipocytes before Fura-2-AM preload. Cellular [Ca^{2+}] was determined by a fluorescence microscopy. Water (vehicle) was used as a negative control.

Fig. 2-3

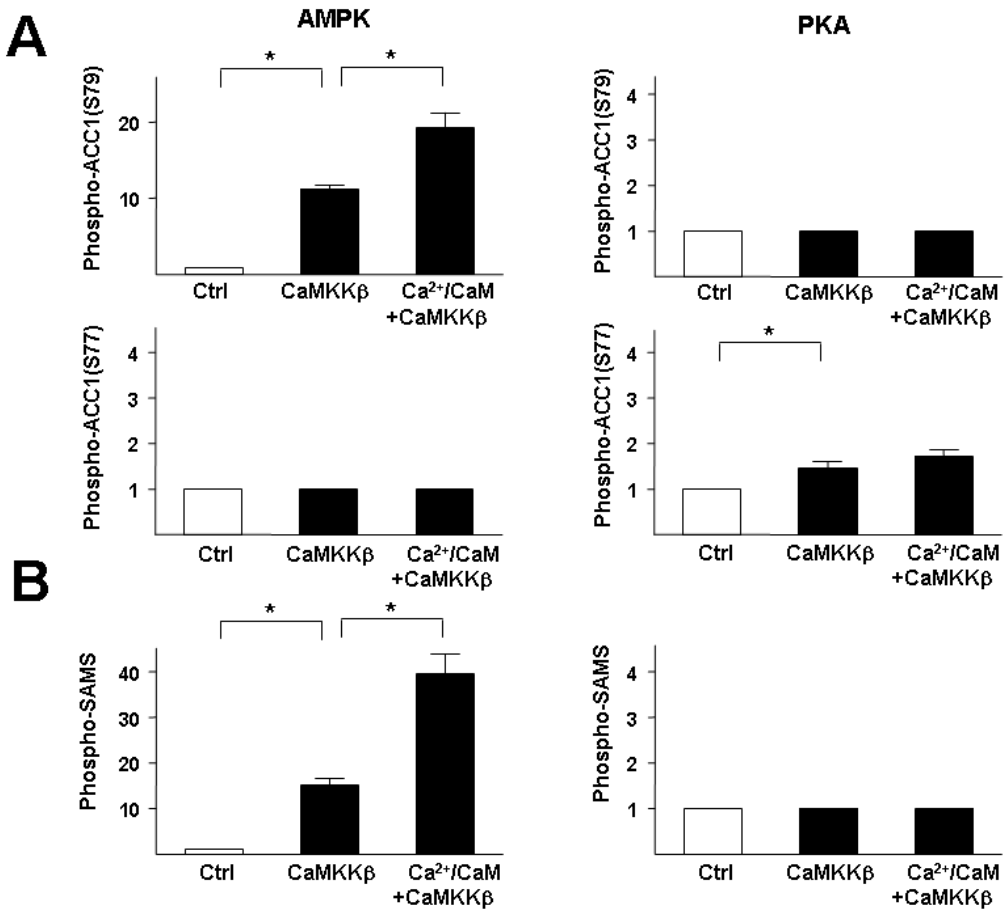

Fig. 2-3. Effect of CaMKKβ alone and with Ca^{2+}/CaM on AMPK and PKA-mediated phosphorylation of ACC1 at S79, ACC1 at S77, and SAMS peptides. The kinase activity of purified GST-AMPKα1 (44 nM) or PKA (95 nM) was determined by mixing 1 mM ACC1 peptide (HMRSSMSGLHLVKQG) (**A**) or SAMS peptide (**B**) with GST-CaMKKβ (46 nM) with or without Ca^{2+} (2 mM)/CaM (2 μM). Nano-LC/MS/MS spectrometry was used to quantify the relative amount of phosphorylation. The fold-change in level of phosphorylated peptide was normalized to that of control (without GST-CaMKKβ) set as 1. The bar graphs represent mean ± SD from 3 independent experiments. *$p < 0.05$ between indicated groups.

Fig. 2-4

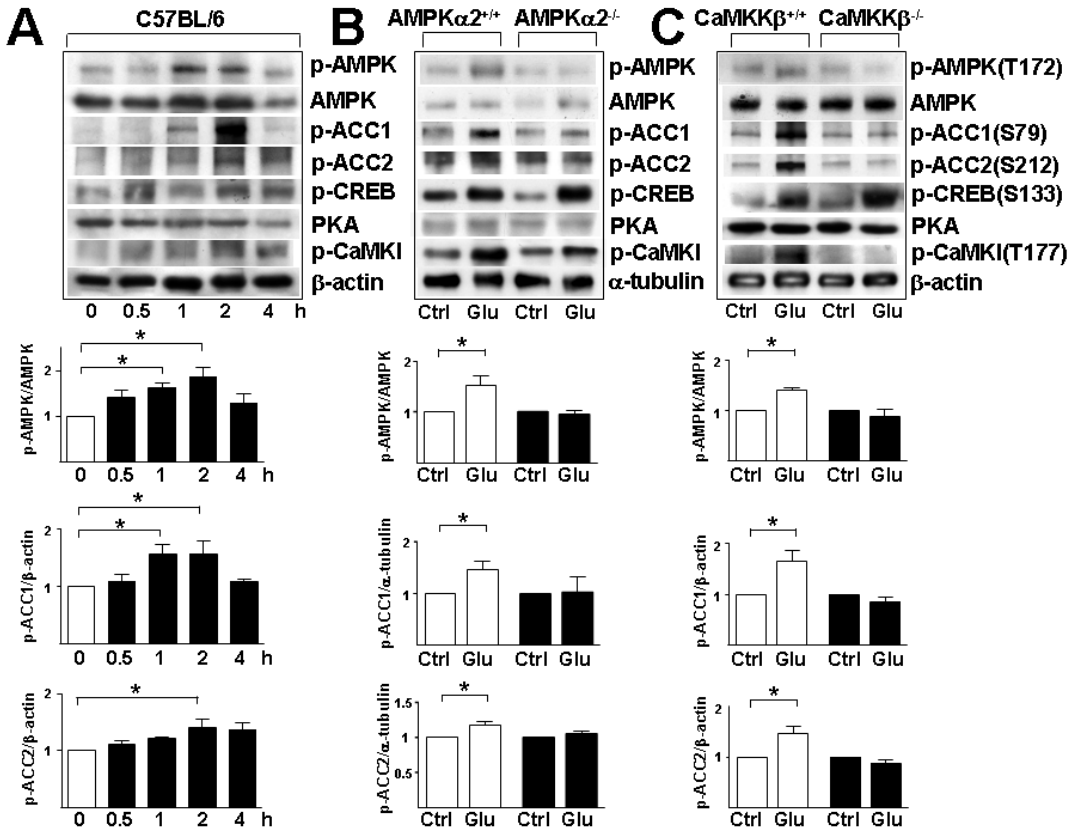

Fig. 2-4. Glucagon-induced ACC1/ACC2 phosphorylation is mediated by CaMKKβ/AMPK in mouse adipose tissue. Glucagon (5 μg/kg) was administered to (**A**) C57BL/6 mice for the indicated times. In (**B**) and (**C**), AMPKα2$^{+/+}$, AMPKα2$^{-/-}$, CaMKKβ$^{+/+}$, and CaMKKβ$^{-/-}$ mice received the same dose of glucagon or 0.2 ml saline for 2 hr. After sacrifice, the tissue extracts of the epididymal fat pads were subjected to Western blotting to reveal the phosphorylation of AMPK T172, ACC1 S79, ACC2 S212, CREB S133, and CaMKI T177. The bar graphs represent densitometry analyses of the ratios of phospho-AMPK T172 to AMPK, and phospho-ACC1 S79 or phospho-ACC2 S212 to β-actin or α-tubulin. Data represent mean ± SEM from three animals, with control groups set as 1. *$p < 0.05$ between indicated groups.

Fig. 2-5

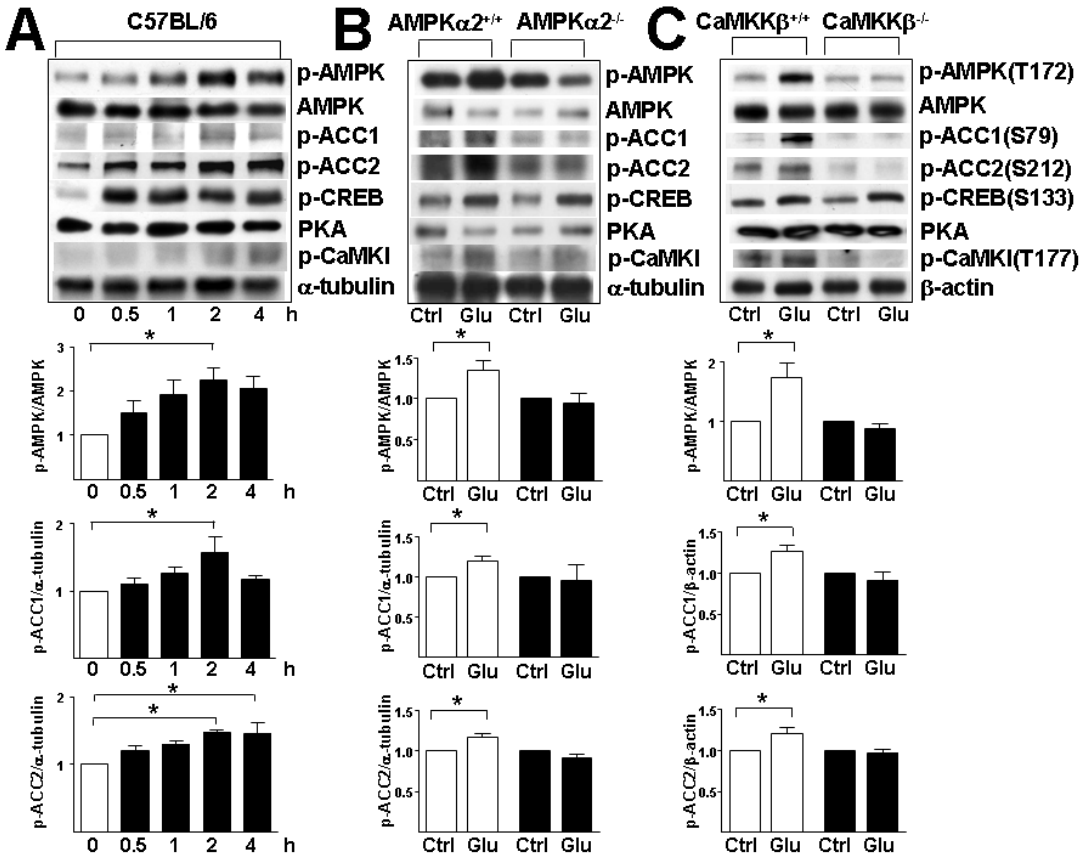

Fig. 2-5. Glucagon-induced ACC1/ACC2 phosphorylation is mediated by CaMKKβ/AMPK in mouse liver. Glucagon (5 μg/kg) was administered to (**A**) C57BL/6 mice for the indicated times. In (**B**) and (**C**), AMPKα2$^{+/+}$, AMPKα2$^{-/-}$, CaMKKβ$^{+/+}$, and CaMKKβ$^{-/-}$ mice received the same dose of glucagon or 0.2 ml saline for 2 hr. After sacrificing, liver extracts were resolved by SDS-PAGE and then subjected to Western blot analysis to reveal the phosphorylation of AMPK T172, ACC1 S79, ACC2 S212, CREB S133, and CaMKI T177. The bar graphs represent densitometry analyses of the ratios of phospho-AMPK T172 to AMPK and phospho-ACC1 S79 or phospho-ACC2 S212 to α-tubulin or β-actin. Data represent mean ± SEM from 3 animals, with control groups set as 1. *p < 0.05 between indicated groups.

Fig. 2-6

A

Mouse ACC1	**$H^{73}M^{74}R^{75}SS^{77}MS^{79}GLHL^{84}$**
Consensus recognition motif for AMPK	**Φ-[β,X]-X-X-S/T-X-X-X-Φ**
Consensus recognition motif for PKA	**R-R-X-S/T**

B **C**

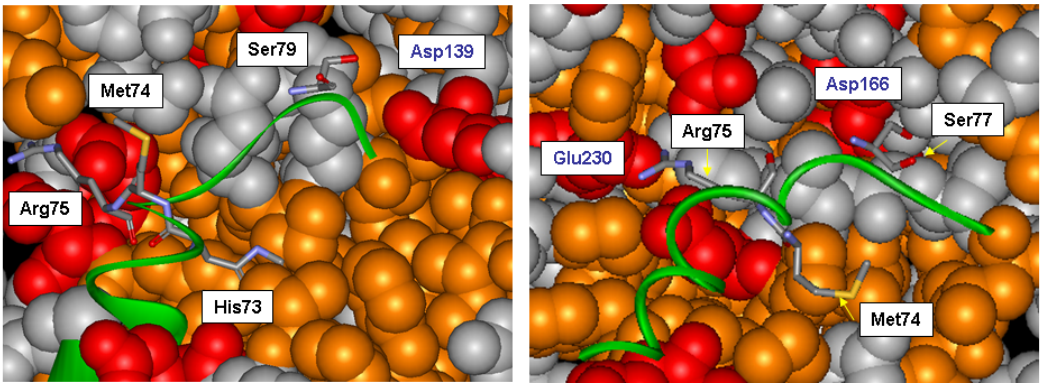

Fig. 2-6. Structure modeling of ACC1 peptide with AMPK or PKA. (**A**) Portion of ACC1 sequence containing S77 and S79, and the consensus recognition motif for AMPK and PKA. (**B**) Model of the peptide around S79 on ACC1 and AMPK. (**C**) Model of the peptide around S77 on ACC1 and PKA. The AMPK or PKA kinase domain is represented as a sphere and the ACC1 peptide is shown in ribbons with the side chains of selected amino acids in stick representation. The interface residues are labeled. (Images were constructed with the help of Dr. Mei-I Su)

Chapter 3

CaMKKβ/AMPK mediated lipogenic activity in adipocytes

3.1 Abstract

Lipid synthesis and storage in adipose tissues contribute to energy homeostasis, which is inversely regulated by activated AMPK. In this chapter, I report that CaMKKβ negatively regulates lipogenesis in adipocytes through its phosphorylation of AMPK. Fasting increases but refeeding decreases the phosphorylation of AMPK and ACC1/ACC2 in CaMKKβ$^{+/+}$ but not CaMKKβ$^{-/-}$ mice. Under *ad libitum* feeding, the increased expression of SREBP-1c-mediated lipogenic gene is concurrent with decreased phosphorylation of AMPK-regulated ACC1/ACC2 in WAT of CaMKKβ$^{-/-}$ mice. In line with the inhibitory role of CaMKKβ in lipid synthesis and storage, CaMKKβ$^{-/-}$ mice exhibit increased body weight, adiposity, and adipocyte hypertrophy, even though their food intake is the same as that of CaMKKβ$^{+/+}$ littermates. Thus, CaMKKβ/AMPK signaling is an important molecular event in physiological regulation of adiposity.

3.2 Introduction

Lipogenesis in WAT is controlled by lipogenic enzymes regulated at both post-translational and transcriptional levels. In chapter 2, I showed that CaMKKβ/AMPK negatively regulates ACC1/ACC2 activity through phosphorylation

in response to glucagon. The transcriptional regulation of lipogenic enzymes, including ACC1, ACC2, FAS, SCD1, and LPL, is mainly through SREBP-1c (2, 31-33, 114). SREBP-1c is negatively regulated by AMPK (101-103), which may be due in part to AMPK phosphorylation of SREBP-1c S372, thus leading to inhibition of both SREBP-1c maturation and expression (54). Therefore, CaMKKβ/AMPK may also regulate lipogenesis at the transcriptional level.

Lipogenesis is regulated by the nutritional environment, such as feeding and fasting. Fasting decreases lipogenic activity in WAT, whereas refeeding restores it. Fasting has been shown to decrease ACC1/ACC2 activity and expression, but the mechanism remains unclear. ACC1/ACC2 activity is mainly controlled by AMPK (20-22), and fasting has been shown to activate AMPK. Therefore, fasting-regulated ACC1/ACC2 activity may be through the CaMKKβ/AMPK pathway. Functioning as the master regulator of lipogenic genes, SREBP-1c is negatively regulated during fasting by several mechanisms. These mechanisms include AMPK phosphorylating SREBP-1c at S372, thus leading to inhibition of SREBP-1c maturation (54), and interferon regulatory factor 4 (IRF4) inhibiting the transcriptional activation of SREBP-1c (100). In this chapter, I examine CaMKKβ/AMPK signaling in the regulation of ACC1/ACC2 activity and expression under fasting, refeeding, and *ad libitum*.

3.3 Materials and Methods

3.3.1 Antibodies and reagents

Antibodies against phospho-AMPKα T172, AMPKα, phospho-ACC1 S79/ACC2 S212, phospho-CREB S133, PKA and α-tubulin, GST-AMPKα, GST-CaMKKβ, and PKA C-α were from Cell Signaling. Anti-CaMKK was from BD Biosciences Pharmingen. Anti-ACC, anti-phospho-CaMKI T177 and anti-β-actin were from Santa Cruz Biotechnology.

3.3.2 Western blot analysis

After treatment, cells were harvested and lysed. After protein quantification, an equal amount of total protein was resolved by 8% SDS-PAGE and then transferred to a PVDF membrane. Samples were immunoblotted with primary antibodies, and then horseradish peroxidase-conjugated secondary antibodies. Bands were visualized by use of an enhanced chemiluminescence detection kit (Amersham Biosciences) and quantified by use of ImageJ.

3.3.3 Animal experiments

The animal experiments were approved by the UCR institutional Animal Care and Use Committee. Twelve-week-old male CaMKKβ$^{+/+}$ and CaMKKβ$^{-/-}$ mice were housed in a 12-hr light/12-hr dark cycle with free access to regular chow unless otherwise described. For fasting and refeeding experiments, mice were fasted for 30 hr or fasted for 30 hr and then refed for 10 hr. Mice had free access to water during

food deprivation. Food intake during refeeding was monitored hourly. At the end of fasting or refeeding, mice were sacrificed, and epididymal fat pads were collected. Serum glucagon and insulin levels were detected by Milliplex Map mouse endocrine panel. Serum levels of total triglycerides (TG) and low-density lipoprotein (LDL) were determined by L-Type TG M and L-Type LDL-C tests (both Wako), respectively. Serum level of total cholesterol (TC) was determined by the Infinity^{TM} Cholesterol Reagent method (Thermo Scientific). Serum levels of high-density lipoprotein (HDL) and very low-density lipoprotein (VLDL) were determined by the Friedwald equation. Mice were fed LabDiet 5001* for 40 weeks. Body weight was measured every week. Body length was measured as nose-to-rump length after euthanasia. Food consumption was monitored every 2 days during 8 days when mice had free access to food and water. Mice were fasted for 14 hr before measurement of basal metabolic rate (BMR), determined by measuring oxygen consumption (ml/min) for 4 hr. For glucose tolerance test (GTT), mice were fasted for 15 hr, and blood glucose levels were determined at 0, 15, 30, 60, and 120 min after intraperitoneal injection of glucose (2 g/kg). For insulin tolerance test (ITT), mice were fasted for 3 hr and then received insulin (1 U/kg) intraperitoneally. Glucose levels were then measured at 0, 15, 30, 60, 90, and 120 min.

3.3.4 Quantitative RT-PCR

Total RNA was isolated by the TRIzol reagent method (Invitrogen). Reverse transcription involved 2 μg total RNA with SuperScript II reverse transcriptase (Invitrogen). Synthesized cDNA was used for real-time quantitative PCR (qPCR) with iQ SYBR Green supermix (Bio-Rad) and the MYQ real-time PCR detection system (Bio-Rad). The primer sequences were for ACC1, TGACAGACTGATCGCAGAGAAAG and TGGAGAGCCCCACACACA; ACC2, CGCTCACCAACAGTAAGGTGG and GCTTGGCAGGGAGTTCCTC; SREBP-1c, GGAGCCATGGATTGCACATT and GGCCCGGGAAGTCACTGT; FAS, GCTGCGGAAACTTCAGGAAAT and AGAGACGTGTCACTCCTGGACTT; SCD1, TTCTTCTCTCACGTGGGTTG and CGGGCTTGTAGTACCTCCTC; LPL, GGGAGTTTGGCTCCAGAGTTT and TGTGTCTTCAGGGGTCCTTAG; GAPDH, AGGCCGGTGCTGAGTATGTC and TGCCTGCTTCACCACCTTCT. The relative abundance of specific mRNAs was normalized to GAPDH mRNA as the invariant control.

3.3.5 Histology and cell size measurement

Fresh epididymal fat pads from CaMKKβ$^{+/+}$ or CaMKKβ$^{-/-}$ mice were embedded in O.C.T. and then frozen 10-μm sections were processed. The specimens were fixed and stained with hematoxylin and eosin. Analysis of more than 350 adipocytes per group in acquired images involved use of ImageJ.

3.3.6 Statistical analysis

Unless indicated, results are expressed as mean ± SEM from three independent experiments. Experiments comparing two groups were analyzed by Student *t* test. Differences among multiple groups were initially evaluated by ANOVA, then Dunnett or Newman-Keuls post-hoc test with GraphPad Prism 4 for Windows (GraphPad Software Inc.). For histological specimens, statistical analysis involved use of SAS 9.0 (SAS Inst.) and two-tailed Wilcoxon Rank Sum test were used to determine the differences. Unless otherwise indicated, $*p<0.05$ was considered statistically significant.

3.4 Results

CaMKKβ is necessary for fasting-induced ACC1/ACC2 phosphorylation *in vivo*

To explore the role of CaMKKβ in adipose tissue under physiological conditions, 12-week old CaMKKβ$^{-/-}$ and their littermate CaMKKβ$^{+/+}$ mice were divided into three groups: fed *ad libitum* (control), fasted for 30 hr, or fasted for 30 hr and then refed for 10 hr before sacrifice. Fasting increased the plasma level of glucagon but decreased that of insulin in CaMKKβ$^{+/+}$ mice. Refeeding restored them to the levels at *ad libitum* (Fig. 1A). In CaMKKβ$^{-/-}$ mice, the fasting/refeeding-induced hormone fluctuations were similar to those in the wild-type, except the glucagon level remained high 10 hr after refeeding. Because of low appetite due to lack of fasting-induced AMPK phosphorylation in the hypothalamus

(67), the reduced amount of food consumed by CaMKKβ$^{-/-}$ mice during refeeding (Fig. 1B) may account in part for the sustained elevated level of glucagon in these animals. In contrast, the insulin surge in these animals caused by refeeding seemed less dependent on the amount of food intake (115, 116). Fasting increased the phosphorylation of AMPK, ACC1, and ACC2 in WAT of CaMKKβ$^{+/+}$ mice, when compared with those under *ad libitum* or after refeeding (Fig. 1C). For CaMKKβ$^{-/-}$ mice, the extent of phosphorylation of the three proteins did not differ among the three metabolic conditions. These results confirm that fasting-induced AMPK and ACC1/ACC2 phosphorylation is mediated by CaMKKβ.

The expression of SREBP-1c and ACC1/ACC2 in WAT is increased in CaMKKβ$^{-/-}$ mice

Because glucagon administration and fasting share a similar pathway to induce AMPK phosphorylation in adipose tissue (Fig. 2-4 and 3-1) and AMPK negatively regulates SREBP-1c (54, 101-103), we compared transcriptional changes of ACC1 and ACC2 and their regulatory transcription factor SREBP-1c in CaMKKβ$^{-/-}$ and wild-type control mice. As expected, under *ad libitum*, mRNA levels of ACC1, ACC2, and SREBP-1c were higher in CaMKKβ$^{-/-}$ than CaMKKβ$^{+/+}$ mice (Fig. 3-2A). Furthermore, the SREBP-1c-regulated FAS and SCD1 mRNA levels were both increased in CaMKKβ$^{-/-}$ mice, which suggests that the expression of lipogenic genes in WAT under *ad libitum* is negatively regulated by CaMKKβ as well (Fig. 3-2A).

Compared with *ad libitum*, fasting reduced the level of ACC1, ACC2, and SREBP-1c mRNA in WAT of both CaMKKβ$^{+/+}$ and CaMKKβ$^{-/-}$ mice (Fig. 3-2B), which indicates that SREBP-1c-regulated adiposity is attenuated under fasting regardless of the presence or absence of CaMKKβ. As compared with fasting, with refeeding, the mRNA levels of ACC1, ACC2, and SREBP-1c were increased more in CaMKKβ$^{+/+}$ than CaMKKβ$^{-/-}$ mice (Fig. 3-2C). The low induction of lipogenic genes in CaMKKβ$^{-/-}$ mice might have been due to less consumed food (Fig. 3-1B). However, CaMKKβ$^{-/-}$ mice restored their appetite and ate even more afterwards. The accumulated food consumption during 24-hr refeeding was comparable between the two groups (data not shown).

Lipogenesis in WAT depends on CaMKKβ

Given the increased expression of genes involved in lipogenesis in CaMKKβ$^{-/-}$ mice under *ad libitum*, I monitored changes in body weight of both CaMKKβ$^{-/-}$ and CaMKKβ$^{+/+}$ mice up to 40 weeks of age. As illustrated in Fig. 3-3A, body weight was greater in CaMKKβ$^{-/-}$ than CaMKKβ$^{+/+}$ mice. Given the comparable body length, liver mass, and daily food intake between the two groups of animals (Fig. 3-4), a higher content of visceral fat seen in CaMKKβ$^{-/-}$ mice accounted for the discrepancy in body weight (Fig. 3-3B). Epididymal fat mass was higher and body fat percentage (sum of epididymal, mesenteric, and perirenal fat weight/body weight) was higher by 2% in CaMKKβ$^{-/-}$ than CaMKKβ$^{+/+}$ mice (Fig. 3-3B). Despite increased epididymal adiposity in CaMKKβ$^{-/-}$ mice, these animals did not show

glucose intolerance or insulin resistance (Fig. 3-5). Histological analysis of epididymal adipose tissue confirmed the increase in adipocyte hypertrophy in CaMKKβ$^{-/-}$ mice (Fig. 3-3C). The increased size of adipocytes was consistent with decreased phosphorylation of AMPK, ACC1, and ACC2 and increased mRNA level of SREBP-1c, ACC1, ACC2, FAS, and SCD1 (Fig. 3-3, D and E).

Of note, the phosphorylation of AMPK, ACC1, and ACC2 was decreased in the liver of CaMKKβ$^{-/-}$ mice (Fig. 2-5C), which suggests that hepatic synthesis of fatty acids was also increased in these animals. When examining the serum lipid profile, I found elevated triglyceride and VLDL contents in CaMKKβ$^{-/-}$ mice, whereas levels of LDL and HDL were normal (Table 1). Increased visceral fat in men has been found associated with increased serum insulin level (117). However, I found comparable levels of serum insulin and glucagon in CaMKKβ$^{-/-}$ and CaMKKβ$^{+/+}$ mice (Fig. 3-3G), which suggests that systemic CaMKKβ ablation did not affect long-term alteration in pancreatic secretion of insulin and glucagon. Therefore, under *ad libitum* in CaMKKβ$^{-/-}$ mice, the lipid accumulation in WAT is largely due to a combination of hepatic production, adipocyte uptake and triglyceride storage.

3.5 Discussion

Lipogenesis is regulated by the nutritional environment, in particular feeding and fasting. Fasting regulates lipogenic activity in WAT at both post-translational and transcriptional levels. The present results demonstrate that fasting-regulated

AMPK, ACC1, and ACC2 phosphorylation in WAT is mediated through CaMKKβ (Fig. 3-1C). Fasting-suppressed lipogenic gene expression is regulated by SREBP-1c in WAT (93, 95). Functioning as the master regulator of lipogenic genes, SREBP-1c is negatively regulated during fasting by several mechanisms. These mechanisms include AMPK phosphorylation of SREBP-1c at S372, thus leading to inhibition of SREBP-1c maturation (54), and interferon regulatory factor 4 (IRF4) inhibition of transcriptional activation of SREBP-1c (100). During fasting, I found that phosphorylation of AMPK, ACC1 and ACC2 in WAT of wild-type mice increased (Fig. 3-1C) with concomitant decrease in the expression of SREBP-1c, ACC1, and ACC2 (Fig. 3-2B). In fasted CaMKKβ$^{-/-}$ mice, the expression of SREBP-1c, ACC1, and ACC2 remained low despite the reduced level of AMPK phosphorylation due to CaMKKβ ablation. Although seemingly paradoxical, these molecular events are physiologically possible. Because the nutritional supply was restricted, the SREBP-1c-mediated lipogenesis in WAT would be inhibited in CaMKKβ$^{-/-}$ mice by pathways other than CaMKKβ/AMPK such as insulin-mediated IRF4. Nonetheless, data for fasted CaMKKβ$^{-/-}$ animals do not negate the negative regulation of lipogenesis in WAT by the CaMKKβ/AMPK pathway in the wild-type.

As the major AMPKK in the central nervous system (CNS), CaMKKβ regulates appetite through AMPK and NPY (67). During refeeding, CaMKKβ$^{-/-}$ mice ingested less food than CaMKKβ$^{+/+}$ mice (Fig. 3-1B), which would be due in part to lower AMPK activity in their hypothalamus (67). Low food intake coincided

with a high plasma glucagon level (Fig. 3-1A) and low expression of SREBP-1c, ACC1, and ACC2 mRNA in the WAT of CaMKKβ$^{-/-}$ mice (Fig. 3-2C). However, CaMKKβ$^{-/-}$ and CaMKKβ$^{+/+}$ mice consumed a similar amount of food at 24 hr after the start of refeeding (data not shown). Therefore, alternative CNS pathways compensated the lack of CaMKKβ/AMPK to restore the appetite at a set point with unrestricted nutrition (i.e., *ad libitum*). However, this pathway becomes a major appetite control mechanism with altered nutritional status (e.g., fasting, starvation, and refeeding).

Although CaMKKβ$^{-/-}$ mice and their wild-type littermates ingested a similar amount of food under *ad libitum* (Fig. 3-4), the phosphorylation level of AMPK, ACC1, and ACC2 was lower and expression level of SREBP-1c, ACC1, ACC2, and other lipogenic genes in WAT higher in CaMKKβ$^{-/-}$ than CaMKKβ$^{+/+}$ mice (Fig. 3-3, D and E). This discrepancy suggests that lower CaMKKβ activity in WAT stimulates lipogenesis, thereby causing epididymal adiposity. Because CaMKKβ is the major AMPKK in the liver and adipocytes, the systemic ablation of CaMKKβ would augment lipogenesis in peripheral tissues without affecting the hypothalamic satiety center, particularly under *ad libitum*. This integrated lipid metabolism is supported by the decreased phosphorylation of AMPK and ACC1/ACC2, augmented lipogenic gene expression in the liver (Fig. 2-5 and 3-6), increased VLDL in circulation (Table 1) and upregulated LPL in WAT (Fig. 3-3E). In addition to increased lipogenesis, BMR was lower in CaMKKβ$^{-/-}$ than CaMKKβ$^{+/+}$ mice (Fig.

3-7), which associates well with decreased ACC2 phosphorylation leading to attenuated lipid oxidation in adipocytes.

Fig. 3-1

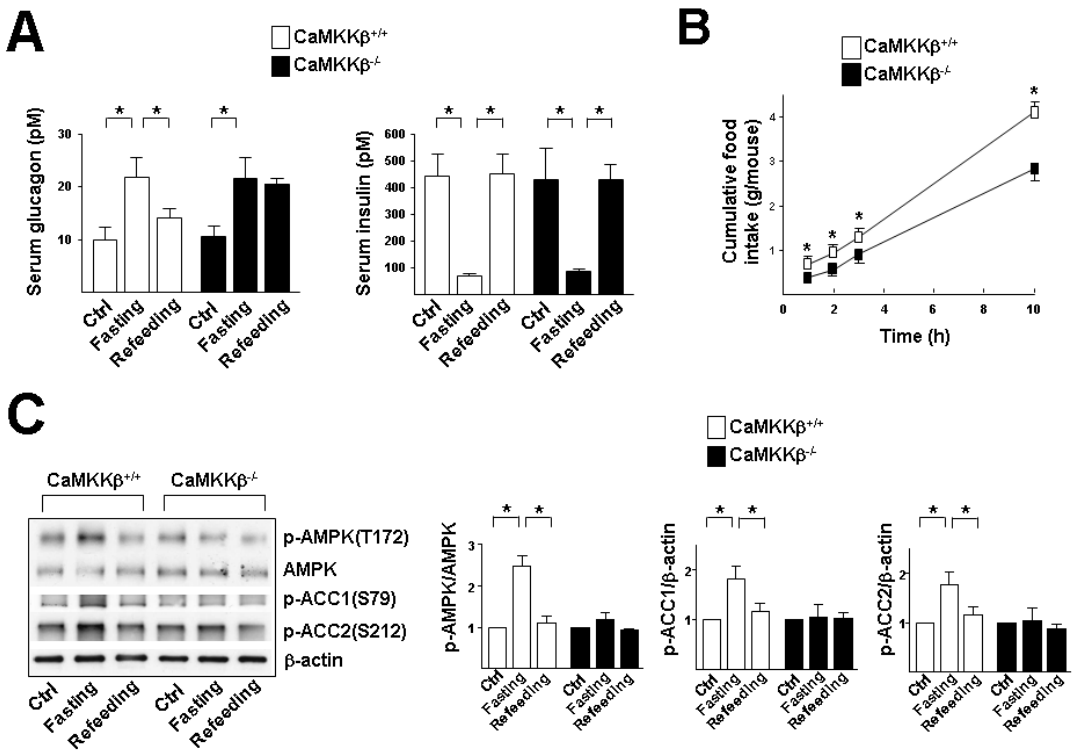

Fig. 3-1. CaMKKβ regulates AMPK and ACC1/ACC2 phosphorylation in mouse adipose tissue during fasting. (**A**) Serum level of glucagon and insulin in CaMKKβ$^{+/+}$ and CaMKKβ$^{-/-}$ mice fed *ad libitum* and those fasted for 30 hr with or without refeeding for 10 hr (n = 4-7). (**B**) The amount of food consumed by CaMKKβ$^{+/+}$ and CaMKKβ$^{-/-}$ mice was monitored during 10-hr refeeding (n = 6). (**C**) Western blot analysis of phosphorylation of AMPK T172, ACC1 S79, and ACC2 S212 in tissue extracts isolated from epididymal fat pads of CaMKKβ$^{+/+}$ and CaMKKβ$^{-/-}$ mice. The bar graphs in panel B represent densitometry analyses of the ratio of phospho-AMPK T172 to AMPK and phospho-ACC1 S79 or phospho-ACC2 S212 to β-actin (n = 3). Data represent mean ± SEM, with control groups set as 1. *$p < 0.05$ between indicated groups.

Fig. 3-2

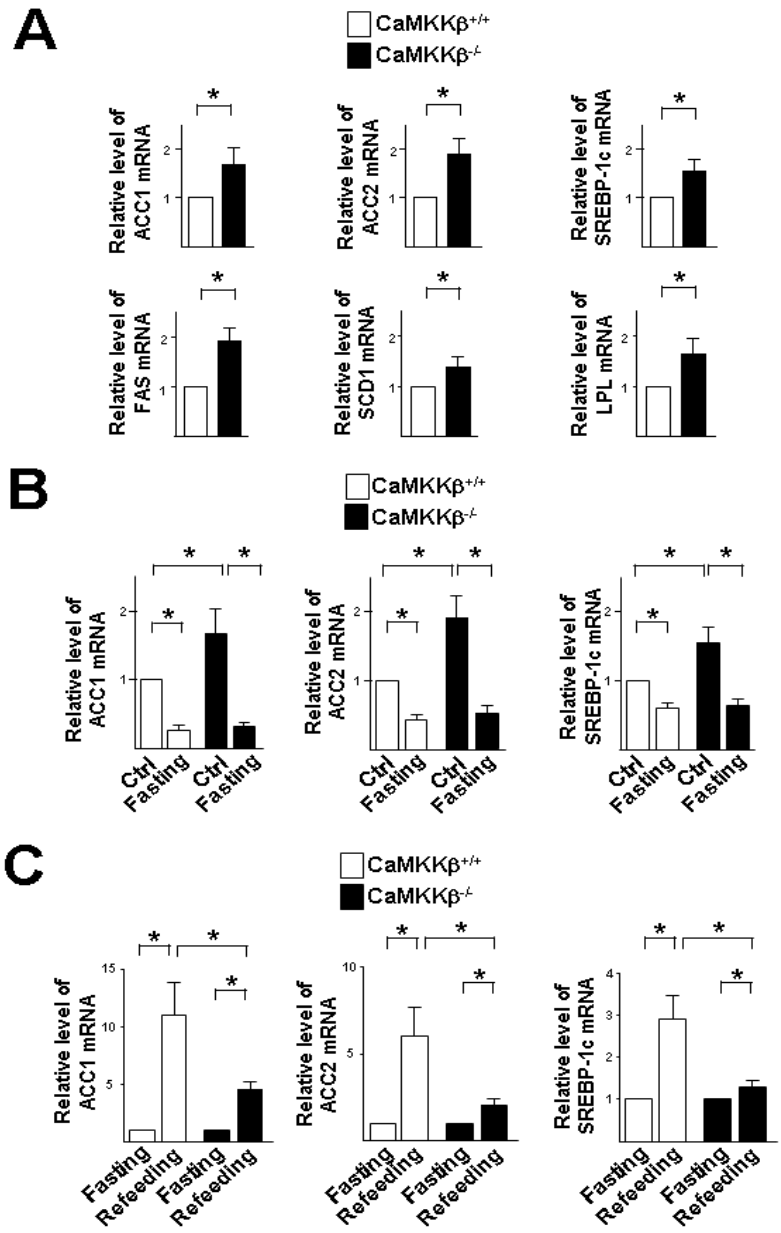

Fig. 3-2. Level of lipogenic genes is upregulated in WAT of CaMKKβ$^{-/-}$ mice. Total RNA was isolated from epididymal fat of CaMKKβ$^{+/+}$ and CaMKKβ$^{-/-}$ mice fed *ad libitum*, subjected to fasting, or fasting and then refeeding (described in Figure 4, n = 6-10 in each group). (**A**) Quantitative RT-PCR of level of ACC1, ACC2, SREBP-1c, FAS, SCD1, and LPL mRNA in CaMKKβ$^{+/+}$ and CaMKKβ$^{-/-}$ mice fed *ad libitum*. (**B** and **C**) Relative levels of ACC1, ACC2, and SREBP-1c mRNA in CaMKKβ$^{+/+}$ and CaMKKβ$^{-/-}$ mice were compared between *ad libitum* and fasting groups as well as fasting and refeeding groups. Data represent mean ± SEM. *$p <$ 0.05 between indicated groups.

Fig. 3-3

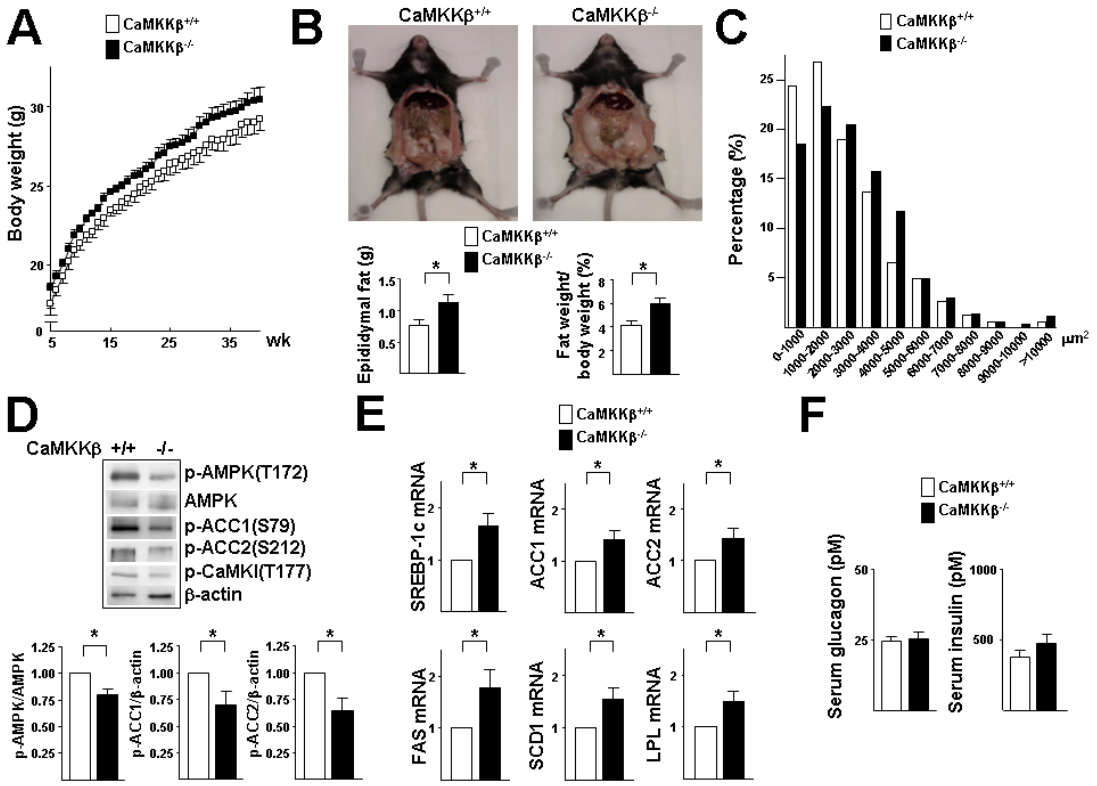

Fig. 3-3. Lipogenesis is enhanced in WAT of CaMKKβ$^{-/-}$ mice. (**A**) Body weight of CaMKKβ$^{+/+}$ (n = 14) and CaMKKβ$^{-/-}$ mice (n = 11) fed *ad libitum* for 40 weeks. (**B**) Photographs of WAT of CaMKKβ$^{+/+}$ and CaMKKβ$^{-/-}$ mice. Epididymal fat weight and combined weight of WAT (sum of epididymal, mesenteric, and perirenal fat weight) as a percentage of total body weight (n = 11-14). (**C**) Comparison of cross-sectional areas of adipocytes from epididymal fat pads of CaMKKβ$^{+/+}$ and CaMKKβ$^{-/-}$ mice. The median area for CaMKKβ$^{+/+}$ was 1939.29 ± 95.69 μm^2, and that for CaMKKβ$^{-/-}$ was 2457.11 ± 113.74 μm^2 (median ± SEM). p<0.01 revealed by Wilcoxon Rank Sum test. (**D**) Phosphorylation of AMPK at T172, ACC1 at S79, ACC2 at S212, and CaMKI at T177 in WAT of CaMKKβ$^{+/+}$ and CaMKKβ$^{-/-}$ mice. The bar graphs represent densitometry analyses of the ratio of phospho-AMPK T172 to AMPK and phospho-ACC1 S79 or phospho-ACC2 S212 to β-actin, averaged from three animals, with wild-type groups set as 1. (**E**) Quantitative RT-PCR of relative mRNA levels of SREBP-1c, ACC1, ACC2, FAS, SCD1, and LPL in WAT (n = 10-14), with wild-type groups set as 1. (**F**) Serum levels of glucagon and insulin in CaMKKβ$^{+/+}$ and CaMKKβ$^{-/-}$ mice (n = 8-14). Data represent mean ± SEM. *p < 0.05 between indicated groups.

Fig. 3-4

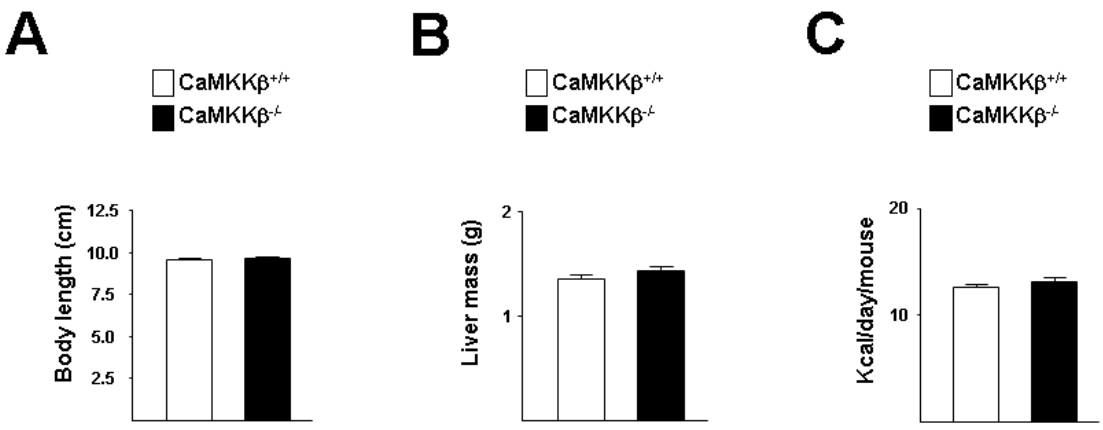

Fig. 3-4. Body length (**A**), liver mass (**B**), and daily food intake (**C**) for CaMKKβ$^{+/+}$ and CaMKKβ$^{-/-}$ mice. Data represent mean ± SEM from 11-14 animals.

Fig. 3-5

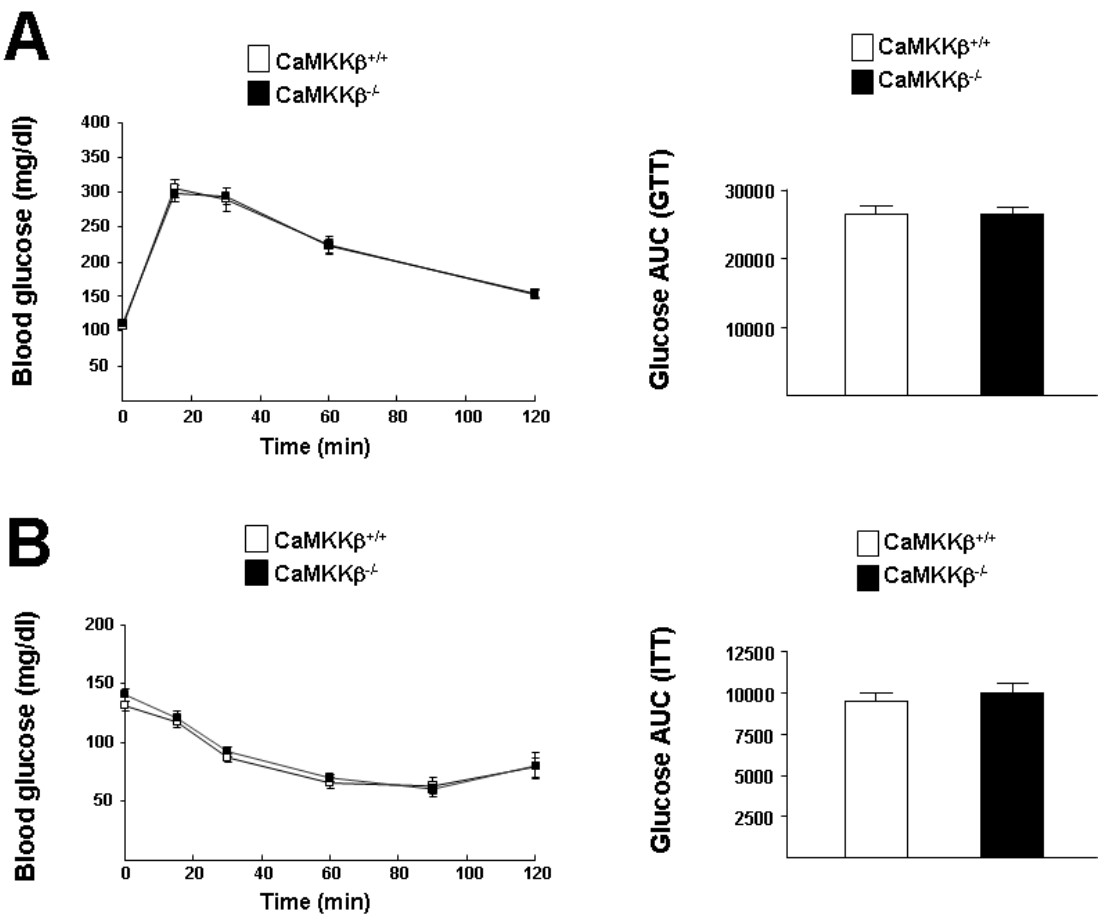

Fig. 3-5. CaMKKβ$^{+/+}$ and CaMKKβ$^{-/-}$ mice show similar glucose tolerance and insulin sensitivity. (**A**) CaMKKβ$^{+/+}$ and CaMKKβ$^{-/-}$ mice were fasted for 15 hr, and then were intraperitoneally injected with glucose (2 g/kg) for GTT. Blood samples were collected from the tail at the indicated times and analyzed for glucose concentration. Data represent mean ± SEM from 12-13 animals. (**B**) CaMKKβ$^{+/+}$ and CaMKKβ$^{-/-}$ mice were fasted for 3 hr, and then were intraperitoneally injected with insulin (1 U/kg). For ITT, blood glucose level was detected at the indicated times. Data are presented as mean ± SEM from 11-12 animals. Data of GTT and ITT were evaluated by calculation of area under the curve (AUC).

Fig. 3-6

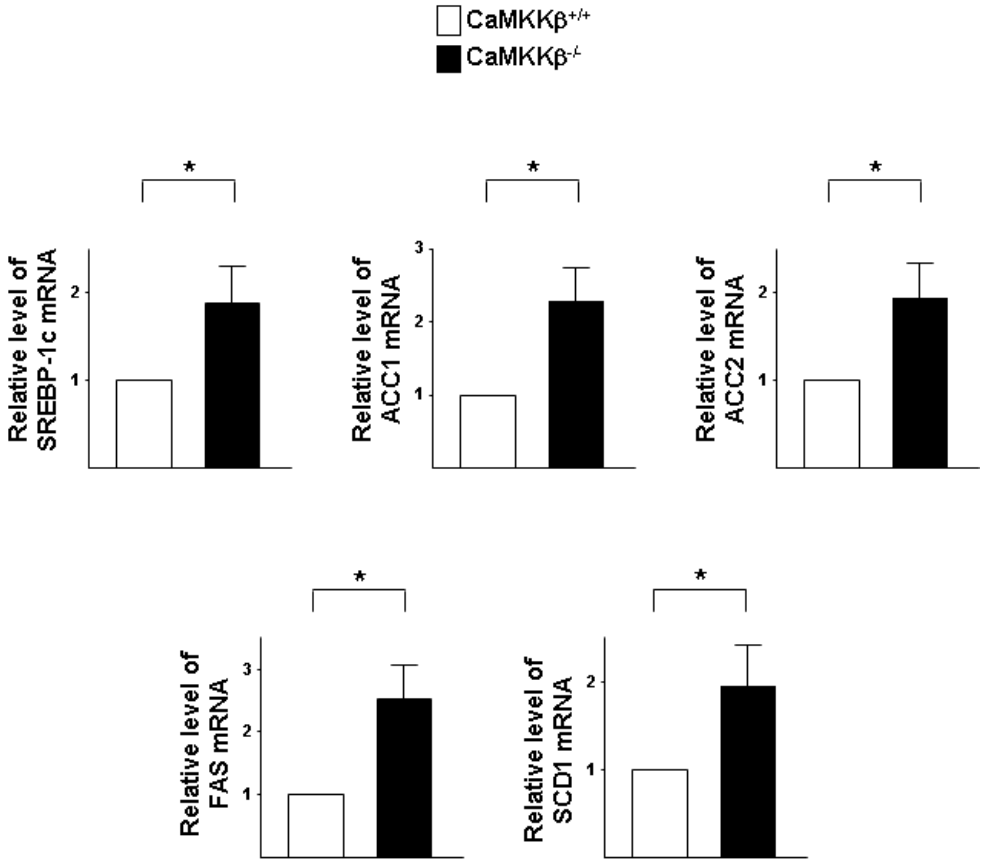

Fig. 3-6. Level of lipogenic genes is upregulated in the liver of CaMKKβ$^{-/-}$ mice. Relative levels of mRNA encoding ACC1, ACC2, SREBP-1c, FAS, and SCD1 in the liver of CaMKKβ$^{+/+}$ and CaMKKβ$^{-/-}$ mice under *ad libitum* were analyzed by quantitative RT-PCR. Data are mean ± SEM averaged from 10-11 animals, with wild-type groups set as 1. *$p < 0.05$ between indicated groups.

Fig. 3-7

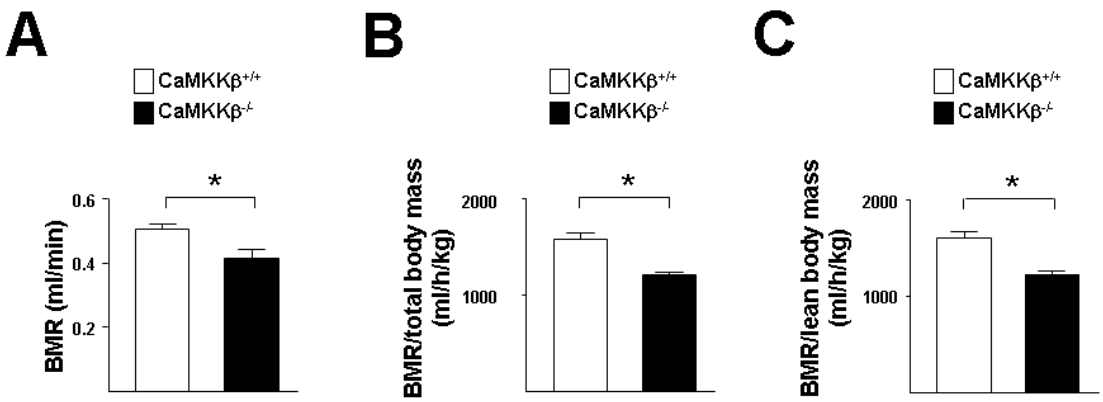

Fig. 3-7. Basal metabolic rate (BMR) for CaMKKβ$^{+/+}$ and CaMKKβ$^{-/-}$ mice. (**A**) Mice were fasted for 14 hr before measurement of BMR. (**B**) and (**C**) are BMR/total body mass and BMR/lean body mass, respectively. Data represent mean ± SEM from 4 animals. *$p < 0.05$ between indicated groups.

Table 1

Serum lipids in CaMKKβ$^{+/+}$ and CaMKKβ$^{-/-}$ mice

	CaMKKβ$^{+/+}$	CaMKKβ$^{-/-}$
TG (mg/dl)	51.36 ± 4.67	69.17 ± 6.87[a]
TC (mg/dl)	94.23 ± 5.64	82.21 ± 6.98
LDL (mg/dl)	18.21 ± 2.51	13.97 ± 2.46
HDL (mg/dl)*	65.75 ± 5.26	54.40 ± 5.52
VLDL (mg/dl)*	10.27 ± 0.93	13.83 ± 1.37[a]

Values are mean ± SEM from 11-13 animals. [a]$p < 0.05$ compared with CaMKKβ$^{+/+}$ mice. *Determined by the Friedwald equation. TG: total triglycerides; TC: total cholesterol; LDL: low-density lipoprotein; HDL: high-density lipoprotein; VLDL: very low-density lipoprotein.

Chapter 4

Conclusions and perspectives

Energy homeostasis at the whole-body level is tightly controlled by myriad biochemical signaling pathways in cells and tissues mediating metabolism such as adipocytes, muscle, liver, and hypothalamus. Regulating multiple metabolic processes, AMPK is widely recognized as a cellular energy gauge (34, 35). In this study, I demonstrated that the CaMKKβ/AMPK pathway in peripheral tissues is important in the regulation of adiposity. The pathway regulates the activities and gene expression of key lipogenic enzymes, ACC1 and ACC2. Because the CaMKKβ/AMPK pathway also regulates appetite in the hypothalamus (67), the coordinated regulation of hypothalamic and peripheral CaMKKβ/AMPK pathways are critical for responding to hormonal and nutrient signals to maintain whole-body energy homeostasis.

4.1 Coordinated regulation of CaMKKβ/AMPK pathway in the periphery

The CaMKKβ/AMPK pathway plays a major role in modulating lipid metabolism in adipocytes at both post-translational and transcriptional events. In this study, I demonstrated that glucagon regulates ACC activity through phosphorylation by the CaMKKβ/AMPK pathway. Also, CaMKKβ/AMPK negatively regulates lipogenic gene expression under *ad libitum* conditions, possibly

through SREBP-1c. These findings emphasize the importance of CaMKKβ/AMPK in regulating lipid metabolism. Fig. 4-1 summarizes the CaMKKβ/AMPK regulation of ACC1/ACC2 in adipocytes.

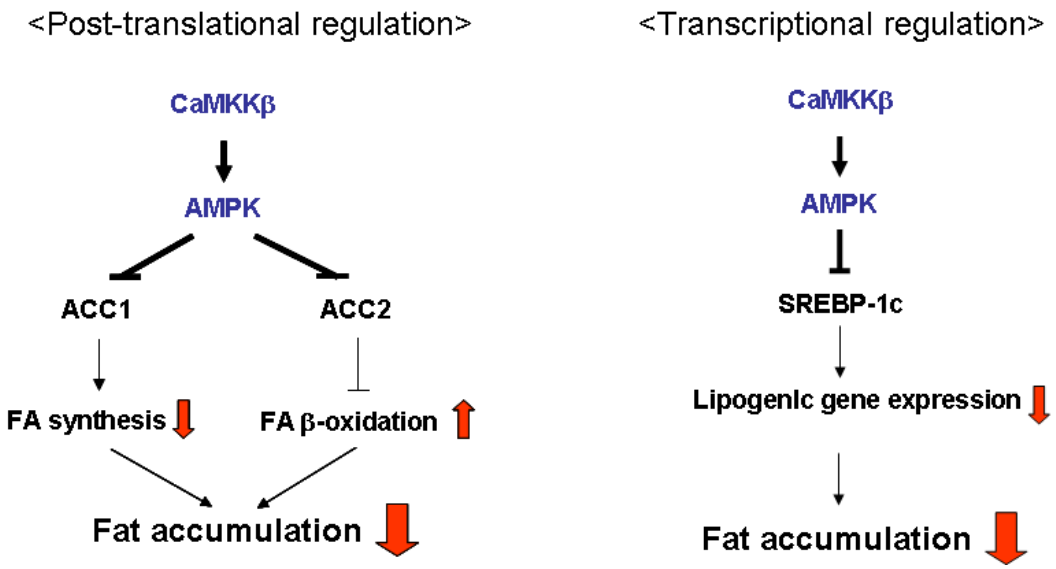

Fig. 4-1. CaMKKβ/AMPK regulation of ACC1/ACC2 in adipocytes. ACC1 and ACC2 are regulated by AMPK at both post-translational and transcriptional levels.

Liver is another important tissue where fatty acid is synthesized. I found the phosphorylation of AMPK, ACC1, and ACC2 decreased and lipogenic gene expression increased in the liver of CaMKKβ$^{-/-}$ mice, which suggests that hepatic synthesis of fatty acids was also increased in these animals. The CaMKKβ/AMPK pathway regulates lipogenic activity in the liver, which in turn affects fat accumulation in adipocytes. This integrated lipid metabolism is supported by the increased level of VLDL in circulation and upregulated LPL in WAT. Fig. 4-2

demonstrates the coordinated regulation of the CaMKKβ/AMPK pathway in the liver and adipocytes.

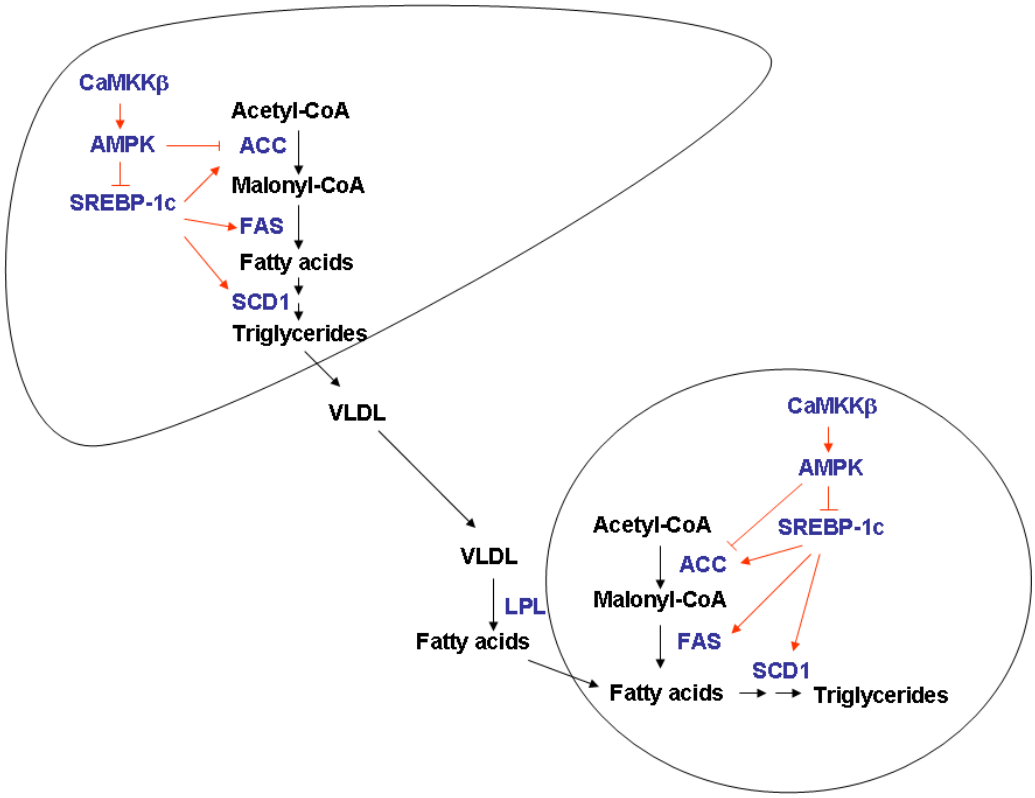

Fig. 4-2. Coordinated regulation of CaMKKβ/AMPK pathway in the liver and adipocytes. Key enzymes involved in lipogenesis are regulated by CaMKKβ/AMPK pathway in the liver and adipocytes.

4.2 CaMKKβ-knockout mice under high-fat diet

As the major AMPKK in the CNS, CaMKKβ regulates appetite through AMPK and NPY (67). CaMKKβ$^{-/-}$ mice under a high-fat diet have lower food intake, thus leading to decreased body weight (Fig. 4-4, C and D), which is consistent with previous findings (67). Although CaMKKβ$^{-/-}$ mice under a high-fat diet have lower body weight, they show increased content of visceral fat (Fig. 4-4, A and B). To

eliminate the effect caused by appetite, CaMKKβ$^{+/+}$ and CaMKKβ$^{-/-}$ mice were fed the same amount of high-fat diet from week 41 to week 60. The body weight was higher for CaMKKβ$^{-/-}$ than CaMKKβ$^{+/+}$ mice at week 60 (Fig. 4-4E). Moreover, CaMKKβ$^{-/-}$ mice under a normal diet exhibited higher body weight and increased accumulation of visceral fat as compared with CaMKKβ$^{+/+}$ mice, although their daily food intake was comparable (Fig. 3-3). Therefore, although CaMKKβ ablation decreases appetite under a high-fat diet, alternative CNS pathways compensate for the lack of CaMKKβ/AMPK to restore the appetite under a normal diet.

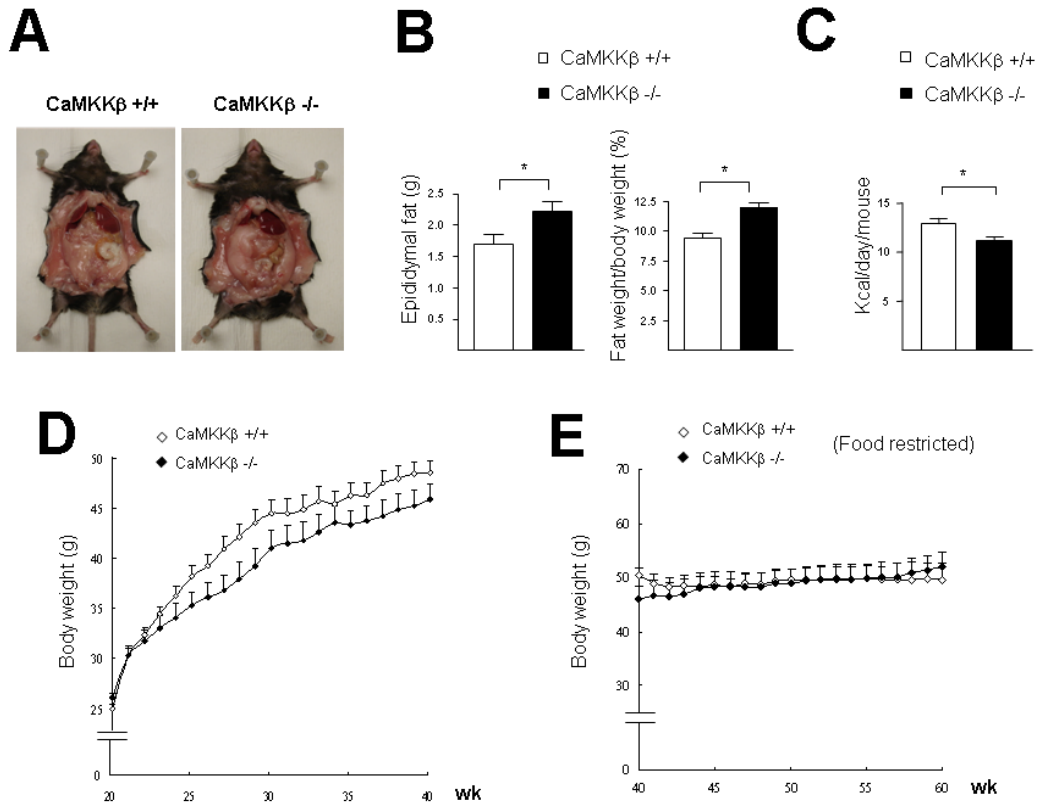

Fig. 4-3. Effect of knocking out CaMKKβ on visceral fat accumulation, food intake, and body weight of mice fed a high-fat diet. (**A**) Photographs of WAT of CaMKKβ$^{+/+}$ and CaMKKβ$^{-/-}$ mice. (**B**) Epididymal fat weight and combined weight of WAT (sum of epididymal, mesenteric, and perirenal fat weight) as a percentage of total body weight. (**C**) Average daily food intake of CaMKKβ$^{+/+}$ and CaMKKβ$^{-/-}$

mice. (**D**) Body weight of CaMKKβ$^{+/+}$ and CaMKKβ$^{-/-}$ mice fed a high-fat diet during weeks 21 to 40. (**E**) Body weight of CaMKKβ$^{+/+}$ and CaMKKβ$^{-/-}$ mice during weeks 41 to 60 when both groups were fed the same amount. To equalize food intake, the CaMKKβ$^{+/+}$ mice were fed only the amount of high-fat diet consumed by the CaMKKβ$^{-/-}$ mice. Data are mean ± SEM. *$p < 0.05$ between indicated groups.

4.3 Generation of tissue-specific CaMKKβ-knockout mice

Because activation of CaMKKβ/AMPK pathway in different tissues leads to different consequences, tissue-specific CaMKKβ-knockout mice are useful to address the specific effect of CaMKKβ in a particular metabolic organ and the consequent functions at the whole-body level. Cre-Lox recombination could be used to delete the loxP-flanked chromosomal CaMKKβ sequence in selected cell types and tissue, such as adipocytes, muscle, liver, and hypothalamus. The Cre protein is a site-specific DNA recombinase that can catalyze the recombination between specific sites in a DNA molecule. These sites, known as loxP sequences, contain specific binding sites for Cre protein. Therefore, one can use adipocyte-, muscle-, liver-, or hypothalamus-expressed Cre mice crossed with LoxP-linked CaMKKβ$^{+/+}$ mice to obtain tissue-specific CaMKKβ$^{-/-}$ mice.

Using hypothalamus-specific CaMKKβ knockout mice, one can study CaMKKβ-regulated appetite under different diets or nutritional status, such as *ad libitum*, fasting, and refeeding. However, using adipocyte-, muscle-, or liver-specific CaMKKβ-knockout mice, the CaMKKβ-regulated lipogenic activity in the periphery can be addressed. The coordinated regulation of lipid and perhaps carbohydrate

metabolism by the hypothalamic and peripheral CaMKKβ/AMPK pathway can thus be demonstrated by comparing hypothalamus- and periphery-specific knockout mice in response to hormonal and/or nutrient signals.

4.4 Metformin activation of the CaMKKβ/AMPK pathway

A translational implication of the enhanced epididymal adiposity in CaMKKβ$^{-/-}$ mice may be the salutary effect of metformin on weight loss (118). Metformin is an oral antidiabetic drug for type 2 diabetes. Many type 2 diabetic patients are overweight or obese, with associated cardiometabolic risk factors. However, many antidiabetic treatments increase body weight; examples are insulin secretagogues (sulphonylureas and meglitinides), thiazolidinediones (TZDs), and insulin itself (119). Metformin has been evaluated in many clinical studies in diverse patient populations and found to decrease body weight (118, 120). Therefore, metformin has been used as a first-line pharmacological therapy in overweight patients (120).

The effect of metformin on hypoglycaemic action has been shown by AMPK activation decreasing glucose production in the liver and increasing glucose utilization in muscle (103). In addition, activation of AMPK is involved in the lipid-lowering effect of metformin leading to decreased ACC activity in the liver (103, 121). Because metformin can induce AMPK and ACC phosphorylation in adipose tissue of rodent models and type II diabetic patients (122, 123), CaMKKβ may be involved in

this effect. Indeed, I found that metformin administration failed to increase AMPK phosphorylation in CaMKKβ$^{-/-}$ MEF-derived adipocytes and WAT of CaMKKβ$^{-/-}$ mice as compared with wild-type controls (Fig. 4-3, A and B). Although LKB1 in the liver is involved in the hypoglycemic action of metformin (124), these results suggest that CaMKKβ in WAT is also targeted by metformin. Interestingly, metformin did not seem to affect AMPK and ACC phosphorylation in the mouse hypothalamus (Fig. 4C). Thus, a possible drug intervention of dysregulated energy storage would be tissue-specific targeting of the CaMKKβ/AMPK in WAT.

To study the long-term effect of metformin-regulated adiposity and body weight change, metformin can be given to the wild-type and CaMKKβ$^{-/-}$ mice for an extended period. The ACC activity and lipogenic gene expression in WAT and liver can then be compared in both groups to show the importance of CaMKKβ in metformin-regulated lipogenesis. In addition, food intake and AMPK phosphorylation in the hypothalamus could be examined to investigate the metformin effect in the CNS.

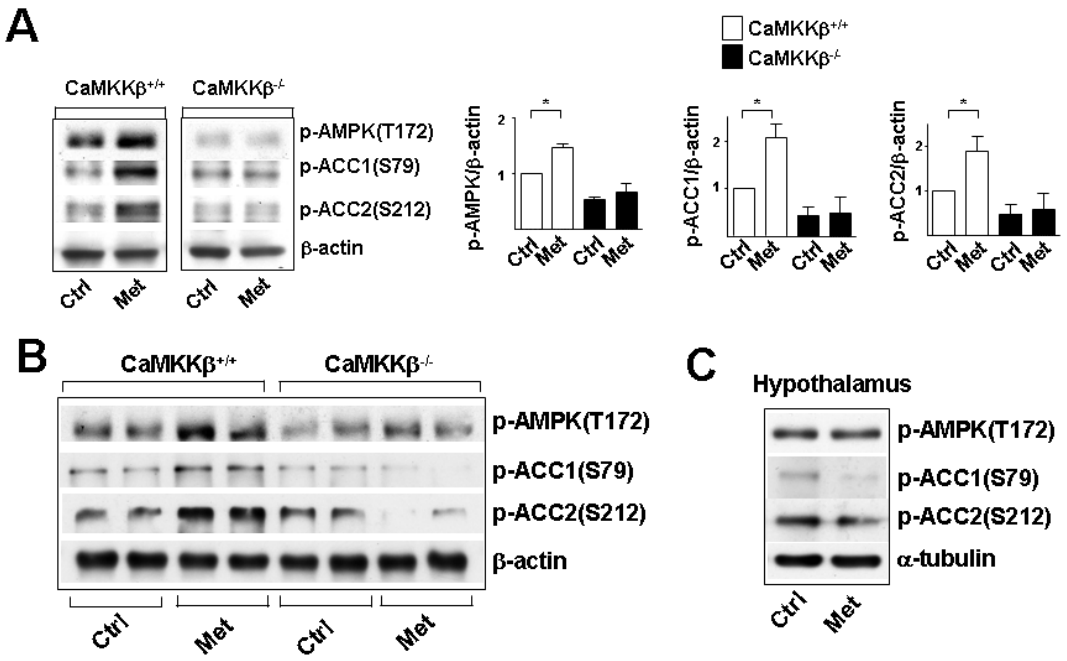

Fig. 4-4. Metformin-induced AMPK and ACC1/ACC2 phosphorylation in adipocytes is mediated by CaMKKβ. (**A**) CaMKKβ$^{+/+}$ and CaMKKβ$^{-/-}$ MEF-derived adipocytes were treated with or without metformin (1 mM) for 2 hr. Cell lysates were analyzed by Western blot analysis. Bar graphs represent mean ± SEM from 3 independent experiments, with control groups set as 1. *$p < 0.05$ between indicated groups. (**B**) CaMKKβ$^{+/+}$ and CaMKKβ$^{-/-}$ mice were administered metformin (500 mg/kg) by oral gavage. At 24 hr, adipose tissue was collected and protein levels were examined by Western blot analysis. (**C**) C57BL/6 mice were treated with oral metformin (500 mg/kg) for 24 hr. Protein levels were examined in hypothalamus tissue by Western blot analysis. (with the help of Drs. Zhen Chen and Wei Sun)

4.5 Summary

This study provides information on the CaMKKβ/AMPK pathway in regulating lipid metabolism in peripheral tissue in mice and implications for regulating adiposity. Hormones, peptides, and nutrients may affect the CaMKKβ/AMPK pathway in both hypothalamus and peripheral tissue. Furthermore, hypothalamic CaMKKβ/AMPK may regulate metabolic pathways in the periphery

through neuronal circuits, and peripheral CaMKKβ/AMPK may also affect hypothalamic signaling. CaMKKβ controls food intake by regulating hypothalamic AMPK, thus leading to the production of the orexigenic hormone NPY, whereas CaMKKβ regulates adiposity by regulating peripheral AMPK and ACC1/ACC2 activity. How the coordinated regulation of the hypothalamic and peripheral CaMKKβ/AMPK cascade responds to multiple stimuli is still unclear. In addition, further delineating this pathway in other tissues or other downstream targets for regulating whole-body energy homeostasis is important. Therefore, tissue-specific CaMKKβ–knockout mice are useful for studying the importance of the CaMKKβ/AMPK pathway outside of adipocytes.

References

1. Wakil, SJ, Stoops, JK, and Joshi, VC. 1983. Fatty acid synthesis and its regulation. *Annu Rev Biochem* 52:537-579.

2. Horton, JD, Goldstein, JL, and Brown, MS. 2002. SREBPs: activators of the complete program of cholesterol and fatty acid synthesis in the liver. *J Clin Invest* 109:1125-1131.

3. Arner, P. 2005. Human fat cell lipolysis: biochemistry, regulation and clinical role. *Best Pract Res Clin Endocrinol Metab* 19:471-482.

4. Lafontan, M, and Langin, D. 2009. Lipolysis and lipid mobilization in human adipose tissue. *Prog Lipid Res* 48:275-297.

5. Large, V, and Arner, P. 1998. Regulation of lipolysis in humans. Pathophysiological modulation in obesity, diabetes, and hyperlipidaemia. *Diabetes Metab* 24:409-418.

6. Oh, W, Abu-Elheiga, L, Kordari, P, Gu, Z, Shaikenov, T, Chirala, SS, and Wakil, SJ. 2005. Glucose and fat metabolism in adipose tissue of acetyl-CoA carboxylase 2 knockout mice. *Proc Natl Acad Sci U S A* 102:1384-1389.

7. Abu-Elheiga, L, Brinkley, WR, Zhong, L, Chirala, SS, Woldegiorgis, G, and Wakil, SJ. 2000. The subcellular localization of acetyl-CoA carboxylase 2. *Proc Natl Acad Sci U S A* 97:1444-1449.

8. Abu-Elheiga, L, Jayakumar, A, Baldini, A, Chirala, SS, and Wakil, SJ. 1995.

Human acetyl-CoA carboxylase: characterization, molecular cloning, and evidence for two isoforms. *Proc Natl Acad Sci U S A* 92:4011-4015.

9. Bianchi, A, Evans, JL, Iverson, AJ, Nordlund, AC, Watts, TD, and Witters, LA. 1990. Identification of an isozymic form of acetyl-CoA carboxylase. *J Biol Chem* 265:1502-1509.

10. Iverson, AJ, Bianchi, A, Nordlund, AC, and Witters, LA. 1990. Immunological analysis of acetyl-CoA carboxylase mass, tissue distribution and subunit composition. *Biochem J* 269:365-371.

11. Abu-Elheiga, L, Almarza-Ortega, DB, Baldini, A, and Wakil, SJ. 1997. Human acetyl-CoA carboxylase 2. Molecular cloning, characterization, chromosomal mapping, and evidence for two isoforms. *J Biol Chem* 272:10669-10677.

12. Trumble, GE, Smith, MA, and Winder, WW. 1995. Purification and characterization of rat skeletal muscle acetyl-CoA carboxylase. *Eur J Biochem* 231:192-198.

13. Harwood, HJ, Jr. 2005. Treating the metabolic syndrome: acetyl-CoA carboxylase inhibition. *Expert Opin Ther Targets* 9:267-281.

14. Kim, KH. 1997. Regulation of mammalian acetyl-coenzyme A carboxylase. *Annu Rev Nutr* 17:77-99.

15. Davies, SP, Sim, AT, and Hardie, DG. 1990. Location and function of three sites phosphorylated on rat acetyl-CoA carboxylase by the AMP-activated protein kinase. *Eur J Biochem* 187:183-190.

16. Haystead, TA, Campbell, DG, and Hardie, DG. 1988. Analysis of sites phosphorylated on acetyl-CoA carboxylase in response to insulin in isolated adipocytes. Comparison with sites phosphorylated by casein kinase-2 and the calmodulin-dependent multiprotein kinase. *Eur J Biochem* 175:347-354.

17. Haystead, TA, and Hardie, DG. 1988. Insulin and phorbol ester stimulate phosphorylation of acetyl-CoA carboxylase at similar sites in isolated adipocytes. Lack of correspondence with sites phosphorylated on the purified enzyme by protein kinase C. *Eur J Biochem* 175:339-345.

18. Munday, MR, Campbell, DG, Carling, D, and Hardie, DG. 1988. Identification by amino acid sequencing of three major regulatory phosphorylation sites on rat acetyl-CoA carboxylase. *Eur J Biochem* 175:331-338.

19. Ha, J, Daniel, S, Broyles, SS, and Kim, KH. 1994. Critical phosphorylation sites for acetyl-CoA carboxylase activity. *J Biol Chem* 269:22162-22168.

20. Davies, SP, Carling, D, Munday, MR, and Hardie, DG. 1992. Diurnal rhythm of phosphorylation of rat liver acetyl-CoA carboxylase by the AMP-activated protein kinase, demonstrated using freeze-clamping. Effects of high fat diets. *Eur J Biochem* 203:615-623.

21. Haystead, TA, Moore, F, Cohen, P, and Hardie, DG. 1990. Roles of the AMP-activated and cyclic-AMP-dependent protein kinases in the adrenaline-induced inactivation of acetyl-CoA carboxylase in rat adipocytes. *Eur J Biochem* 187:199-205.

22. Sim, AT, and Hardie, DG. 1988. The low activity of acetyl-CoA carboxylase in basal and glucagon-stimulated hepatocytes is due to phosphorylation by the AMP-activated protein kinase and not cyclic AMP-dependent protein kinase. *FEBS Lett* 233:294-298.

23. Hutber, CA, Hardie, DG, and Winder, WW. 1997. Electrical stimulation inactivates muscle acetyl-CoA carboxylase and increases AMP-activated protein kinase. *Am J Physiol* 272:E262-266.

24. Winder, WW, Wilson, HA, Hardie, DG, Rasmussen, BB, Hutber, CA, Call, GB, Clayton, RD, Conley, LM, Yoon, S, and Zhou, B. 1997. Phosphorylation of rat muscle acetyl-CoA carboxylase by AMP-activated protein kinase and protein kinase A. *J Appl Physiol* 82:219-225.

25. Winz, R, Hess, D, Aebersold, R, and Brownsey, RW. 1994. Unique structural features and differential phosphorylation of the 280-kDa component (isozyme) of rat liver acetyl-CoA carboxylase. *J Biol Chem* 269:14438-14445.

26. Mao, J, Chirala, SS, and Wakil, SJ. 2003. Human acetyl-CoA carboxylase 1 gene: presence of three promoters and heterogeneity at the 5'-untranslated mRNA region. *Proc Natl Acad Sci U S A* 100:7515-7520.

27. Zhang, Y, Yin, L, and Hillgartner, FB. 2003. SREBP-1 integrates the actions of thyroid hormone, insulin, cAMP, and medium-chain fatty acids on ACCalpha transcription in hepatocytes. *J Lipid Res* 44:356-368.

28. Shimomura, I, Bashmakov, Y, and Horton, JD. 1999. Increased levels of

nuclear SREBP-1c associated with fatty livers in two mouse models of diabetes mellitus. *J Biol Chem* 274:30028-30032.

29. Barber, MC, Price, NT, and Travers, MT. 2005. Structure and regulation of acetyl-CoA carboxylase genes of metazoa. *Biochim Biophys Acta* 1733:1-28.

30. Wolfrum, C, Asilmaz, E, Luca, E, Friedman, JM, and Stoffel, M. 2004. Foxa2 regulates lipid metabolism and ketogenesis in the liver during fasting and in diabetes. *Nature* 432:1027-1032.

31. Boizard, M, Le Liepvre, X, Lemarchand, P, Foufelle, F, Ferre, P, and Dugail, I. 1998. Obesity-related overexpression of fatty-acid synthase gene in adipose tissue involves sterol regulatory element-binding protein transcription factors. *J Biol Chem* 273:29164-29171.

32. Kim, JB, Sarraf, P, Wright, M, Yao, KM, Mueller, E, Solanes, G, Lowell, BB, and Spiegelman, BM. 1998. Nutritional and insulin regulation of fatty acid synthetase and leptin gene expression through ADD1/SREBP1. *J Clin Invest* 101:1-9.

33. Latasa, MJ, Moon, YS, Kim, KH, and Sul, HS. 2000. Nutritional regulation of the fatty acid synthase promoter in vivo: sterol regulatory element binding protein functions through an upstream region containing a sterol regulatory element. *Proc Natl Acad Sci U S A* 97:10619-10624.

34. Carling, D. 2004. The AMP-activated protein kinase cascade--a unifying system for energy control. *Trends Biochem Sci* 29:18-24.

35. Hardie, DG. 2003. Minireview: the AMP-activated protein kinase cascade: the key sensor of cellular energy status. *Endocrinology* 144:5179-5183.

36. Carling, D, Fryer, LG, Woods, A, Daniel, T, Jarvie, SL, and Whitrow, H. 2003. Bypassing the glucose/fatty acid cycle: AMP-activated protein kinase. *Biochem Soc Trans* 31:1157-1160.

37. Merrill, GF, Kurth, EJ, Hardie, DG, and Winder, WW. 1997. AICA riboside increases AMP-activated protein kinase, fatty acid oxidation, and glucose uptake in rat muscle. *Am J Physiol* 273:E1107-1112.

38. Mu, J, Barton, ER, and Birnbaum, MJ. 2003. Selective suppression of AMP-activated protein kinase in skeletal muscle: update on 'lazy mice'. *Biochem Soc Trans* 31:236-241.

39. Mu, J, Brozinick, JT, Jr., Valladares, O, Bucan, M, and Birnbaum, MJ. 2001. A role for AMP-activated protein kinase in contraction- and hypoxia-regulated glucose transport in skeletal muscle. *Mol Cell* 7:1085-1094.

40. Samari, HR, Moller, MT, Holden, L, Asmyhr, T, and Seglen, PO. 2005. Stimulation of hepatocytic AMP-activated protein kinase by okadaic acid and other autophagy-suppressive toxins. *Biochem J* 386:237-244.

41. Sambandam, N, and Lopaschuk, GD. 2003. AMP-activated protein kinase (AMPK) control of fatty acid and glucose metabolism in the ischemic heart. *Prog Lipid Res* 42:238-256.

42. Andersson, U, Filipsson, K, Abbott, CR, Woods, A, Smith, K, Bloom, SR,

Carling, D, and Small, CJ. 2004. AMP-activated protein kinase plays a role in the control of food intake. *J Biol Chem* 279:12005-12008.

43. Han, SM, Namkoong, C, Jang, PG, Park, IS, Hong, SW, Katakami, H, Chun, S, Kim, SW, Park, JY, Lee, KU, et al. 2005. Hypothalamic AMP-activated protein kinase mediates counter-regulatory responses to hypoglycaemia in rats. *Diabetologia* 48:2170-2178.

44. Kim, EK, Miller, I, Aja, S, Landree, LE, Pinn, M, McFadden, J, Kuhajda, FP, Moran, TH, and Ronnett, GV. 2004. C75, a fatty acid synthase inhibitor, reduces food intake via hypothalamic AMP-activated protein kinase. *J Biol Chem* 279:19970-19976.

45. Kola, B, Hubina, E, Tucci, SA, Kirkham, TC, Garcia, EA, Mitchell, SE, Williams, LM, Hawley, SA, Hardie, DG, Grossman, AB, et al. 2005. Cannabinoids and ghrelin have both central and peripheral metabolic and cardiac effects via AMP-activated protein kinase. *J Biol Chem* 280:25196-25201.

46. Minokoshi, Y, Alquier, T, Furukawa, N, Kim, YB, Lee, A, Xue, B, Mu, J, Foufelle, F, Ferre, P, Birnbaum, MJ, et al. 2004. AMP-kinase regulates food intake by responding to hormonal and nutrient signals in the hypothalamus. *Nature* 428:569-574.

47. Luo, Z, Saha, AK, Xiang, X, and Ruderman, NB. 2005. AMPK, the metabolic syndrome and cancer. *Trends Pharmacol Sci* 26:69-76.

48. Hardie, DG. 2004. The AMP-activated protein kinase pathway--new players upstream and downstream. *J Cell Sci* 117:5479-5487.

49. Sullivan, JE, Brocklehurst, KJ, Marley, AE, Carey, F, Carling, D, and Beri, RK. 1994. Inhibition of lipolysis and lipogenesis in isolated rat adipocytes with AICAR, a cell-permeable activator of AMP-activated protein kinase. *FEBS Lett* 353:33-36.

50. Daval, M, Diot-Dupuy, F, Bazin, R, Hainault, I, Viollet, B, Vaulont, S, Hajduch, E, Ferre, P, and Foufelle, F. 2005. Anti-lipolytic action of AMP-activated protein kinase in rodent adipocytes. *J Biol Chem* 280:25250-25257.

51. Daval, M, Foufelle, F, and Ferre, P. 2006. Functions of AMP-activated protein kinase in adipose tissue. *J Physiol* 574:55-62.

52. Kola, B, Boscaro, M, Rutter, GA, Grossman, AB, and Korbonits, M. 2006. Expanding role of AMPK in endocrinology. *Trends Endocrinol Metab* 17:205-215.

53. Villena, JA, Viollet, B, Andreelli, F, Kahn, A, Vaulont, S, and Sul, HS. 2004. Induced adiposity and adipocyte hypertrophy in mice lacking the AMP-activated protein kinase-alpha2 subunit. *Diabetes* 53:2242-2249.

54. Li, Y, Xu, S, Mihaylova, MM, Zheng, B, Hou, X, Jiang, B, Park, O, Luo, Z, Lefai, E, Shyy, JY, et al. AMPK phosphorylates and inhibits SREBP activity to attenuate hepatic steatosis and atherosclerosis in diet-induced insulin-resistant

mice. *Cell Metab* 13:376-388.

55. Woods, A, Cheung, PC, Smith, FC, Davison, MD, Scott, J, Beri, RK, and Carling, D. 1996. Characterization of AMP-activated protein kinase beta and gamma subunits. Assembly of the heterotrimeric complex in vitro. *J Biol Chem* 271:10282-10290.

56. Hardie, DG, and Carling, D. 1997. The AMP-activated protein kinase--fuel gauge of the mammalian cell? *Eur J Biochem* 246:259-273.

57. Cheung, PC, Salt, IP, Davies, SP, Hardie, DG, and Carling, D. 2000. Characterization of AMP-activated protein kinase gamma-subunit isoforms and their role in AMP binding. *Biochem J* 346 Pt 3:659-669.

58. Stapleton, D, Mitchelhill, KI, Gao, G, Widmer, J, Michell, BJ, Teh, T, House, CM, Fernandez, CS, Cox, T, Witters, LA, et al. 1996. Mammalian AMP-activated protein kinase subfamily. *J Biol Chem* 271:611-614.

59. Verhoeven, AJ, Woods, A, Brennan, CH, Hawley, SA, Hardie, DG, Scott, J, Beri, RK, and Carling, D. 1995. The AMP-activated protein kinase gene is highly expressed in rat skeletal muscle. Alternative splicing and tissue distribution of the mRNA. *Eur J Biochem* 228:236-243.

60. Hawley, SA, Boudeau, J, Reid, JL, Mustard, KJ, Udd, L, Makela, TP, Alessi, DR, and Hardie, DG. 2003. Complexes between the LKB1 tumor suppressor, STRAD alpha/beta and MO25 alpha/beta are upstream kinases in the AMP-activated protein kinase cascade. *J Biol* 2:28.

61. Woods, A, Johnstone, SR, Dickerson, K, Leiper, FC, Fryer, LG, Neumann, D, Schlattner, U, Wallimann, T, Carlson, M, and Carling, D. 2003. LKB1 is the upstream kinase in the AMP-activated protein kinase cascade. *Curr Biol* 13:2004-2008.

62. Matejkova, O, Mustard, KJ, Sponarova, J, Flachs, P, Rossmeisl, M, Miksik, I, Thomason-Hughes, M, Grahame Hardie, D, and Kopecky, J. 2004. Possible involvement of AMP-activated protein kinase in obesity resistance induced by respiratory uncoupling in white fat. *FEBS Lett* 569:245-248.

63. Sakamoto, K, McCarthy, A, Smith, D, Green, KA, Grahame Hardie, D, Ashworth, A, and Alessi, DR. 2005. Deficiency of LKB1 in skeletal muscle prevents AMPK activation and glucose uptake during contraction. *EMBO J* 24:1810-1820.

64. Shaw, RJ, Kosmatka, M, Bardeesy, N, Hurley, RL, Witters, LA, DePinho, RA, and Cantley, LC. 2004. The tumor suppressor LKB1 kinase directly activates AMP-activated kinase and regulates apoptosis in response to energy stress. *Proc Natl Acad Sci U S A* 101:3329-3335.

65. Hawley, SA, Selbert, MA, Goldstein, EG, Edelman, AM, Carling, D, and Hardie, DG. 1995. 5'-AMP activates the AMP-activated protein kinase cascade, and Ca2+/calmodulin activates the calmodulin-dependent protein kinase I cascade, via three independent mechanisms. *J Biol Chem* 270:27186-27191.

66. Towler, MC, and Hardie, DG. 2007. AMP-activated protein kinase in

metabolic control and insulin signaling. *Circ Res* 100:328-341.

67. Anderson, KA, Ribar, TJ, Lin, F, Noeldner, PK, Green, MF, Muehlbauer, MJ, Witters, LA, Kemp, BE, and Means, AR. 2008. Hypothalamic CaMKK2 contributes to the regulation of energy balance. *Cell Metab* 7:377-388.

68. Angel, A, Desai, K, and Halperin, ML. 1971. Free fatty acid and ATP levels in adipocytes during lipolysis. *Metabolism* 20:87-99.

69. Issad, T, Combettes, M, and Ferre, P. 1995. Isoproterenol inhibits insulin-stimulated tyrosine phosphorylation of the insulin receptor without increasing its serine/threonine phosphorylation. *Eur J Biochem* 234:108-115.

70. Gormand, A, Henriksson, E, Strom, K, Jensen, TE, Sakamoto, K, and Goransson, O. Regulation of AMP-activated protein kinase by LKB1 and CaMKK in adipocytes. *J Cell Biochem* 112:1364-1375.

71. Tokumitsu, H, Enslen, H, and Soderling, TR. 1995. Characterization of a Ca2+/calmodulin-dependent protein kinase cascade. Molecular cloning and expression of calcium/calmodulin-dependent protein kinase kinase. *J Biol Chem* 270:19320-19324.

72. Schumacher, AM, Schavocky, JP, Velentza, AV, Mirzoeva, S, and Watterson, DM. 2004. A calmodulin-regulated protein kinase linked to neuron survival is a substrate for the calmodulin-regulated death-associated protein kinase. *Biochemistry* 43:8116-8124.

73. Hawley, SA, Pan, DA, Mustard, KJ, Ross, L, Bain, J, Edelman, AM,

Frenguelli, BG, and Hardie, DG. 2005. Calmodulin-dependent protein kinase kinase-beta is an alternative upstream kinase for AMP-activated protein kinase. *Cell Metab* 2:9-19.

74. Hurley, RL, Anderson, KA, Franzone, JM, Kemp, BE, Means, AR, and Witters, LA. 2005. The Ca2+/calmodulin-dependent protein kinase kinases are AMP-activated protein kinase kinases. *J Biol Chem* 280:29060-29066.

75. Woods, A, Dickerson, K, Heath, R, Hong, SP, Momcilovic, M, Johnstone, SR, Carlson, M, and Carling, D. 2005. Ca2+/calmodulin-dependent protein kinase kinase-beta acts upstream of AMP-activated protein kinase in mammalian cells. *Cell Metab* 2:21-33.

76. Robson, NA, Clegg, RA, and Zammit, VA. 1984. Regulation of peripheral lipogenesis by glucagon. Inability of the hormone to inhibit lipogenesis in rat mammary acini in vitro in the presence or absence of agents which alter its effects on adipocytes. *Biochem J* 217:743-749.

77. Saltiel, AR, and Kahn, CR. 2001. Insulin signalling and the regulation of glucose and lipid metabolism. *Nature* 414:799-806.

78. Zammit, VA, and Corstorphine, CG. 1982. Inhibition of acetyl-CoA carboxylase activity in isolated rat adipocytes incubated with glucagon. Interactions with the effects of insulin, adrenaline and adenosine deaminase. *Biochem J* 208:783-788.

79. Unger, RH, and Orci, L. 1976. Physiology and pathophysiology of glucagon.

Physiol Rev 56:778-826.

80. Taborsky, GJ, Jr. The physiology of glucagon. *J Diabetes Sci Technol* 4:1338-1344.

81. Heppner, KM, Habegger, KM, Day, J, Pfluger, PT, Perez-Tilve, D, Ward, B, Gelfanov, V, Woods, SC, DiMarchi, R, and Tschop, M. Glucagon regulation of energy metabolism. *Physiol Behav* 100:545-548.

82. Svoboda, M, Tastenoy, M, Vertongen, P, and Robberecht, P. 1994. Relative quantitative analysis of glucagon receptor mRNA in rat tissues. *Mol Cell Endocrinol* 105:131-137.

83. Jiang, G, and Zhang, BB. 2003. Glucagon and regulation of glucose metabolism. *Am J Physiol Endocrinol Metab* 284:E671-678.

84. Burcelin, R, Katz, EB, and Charron, MJ. 1996. Molecular and cellular aspects of the glucagon receptor: role in diabetes and metabolism. *Diabetes Metab* 22:373-396.

85. Christophe, J. 1995. Glucagon receptors: from genetic structure and expression to effector coupling and biological responses. *Biochim Biophys Acta* 1241:45-57.

86. Xu, Y, and Xie, X. 2009. Glucagon receptor mediates calcium signaling by coupling to G alpha q/11 and G alpha i/o in HEK293 cells. *J Recept Signal Transduct Res* 29:318-325.

87. Holland, R, Hardie, DG, Clegg, RA, and Zammit, VA. 1985. Evidence that

glucagon-mediated inhibition of acetyl-CoA carboxylase in isolated adipocytes involves increased phosphorylation of the enzyme by cyclic AMP-dependent protein kinase. *Biochem J* 226:139-145.

88. Holland, R, Witters, LA, and Hardie, DG. 1984. Glucagon inhibits fatty acid synthesis in isolated hepatocytes via phosphorylation of acetyl-CoA carboxylase by cyclic-AMP-dependent protein kinase. *Eur J Biochem* 140:325-333.

89. Munday, MR. 2002. Regulation of mammalian acetyl-CoA carboxylase. *Biochem Soc Trans* 30:1059-1064.

90. Raghow, R, Yellaturu, C, Deng, X, Park, EA, and Elam, MB. 2008. SREBPs: the crossroads of physiological and pathological lipid homeostasis. *Trends Endocrinol Metab* 19:65-73.

91. Hua, X, Wu, J, Goldstein, JL, Brown, MS, and Hobbs, HH. 1995. Structure of the human gene encoding sterol regulatory element binding protein-1 (SREBF1) and localization of SREBF1 and SREBF2 to chromosomes 17p11.2 and 22q13. *Genomics* 25:667-673.

92. Miserez, AR, Cao, G, Probst, LC, and Hobbs, HH. 1997. Structure of the human gene encoding sterol regulatory element binding protein 2 (SREBF2). *Genomics* 40:31-40.

93. Shimano, H, Horton, JD, Shimomura, I, Hammer, RE, Brown, MS, and Goldstein, JL. 1997. Isoform 1c of sterol regulatory element binding protein is

less active than isoform 1a in livers of transgenic mice and in cultured cells. *J Clin Invest* 99:846-854.

94. Shimomura, I, Shimano, H, Horton, JD, Goldstein, JL, and Brown, MS. 1997. Differential expression of exons 1a and 1c in mRNAs for sterol regulatory element binding protein-1 in human and mouse organs and cultured cells. *J Clin Invest* 99:838-845.

95. Kim, JB, and Spiegelman, BM. 1996. ADD1/SREBP1 promotes adipocyte differentiation and gene expression linked to fatty acid metabolism. *Genes Dev* 10:1096-1107.

96. Foretz, M, Guichard, C, Ferre, P, and Foufelle, F. 1999. Sterol regulatory element binding protein-1c is a major mediator of insulin action on the hepatic expression of glucokinase and lipogenesis-related genes. *Proc Natl Acad Sci U S A* 96:12737-12742.

97. Foretz, M, Pacot, C, Dugail, I, Lemarchand, P, Guichard, C, Le Liepvre, X, Berthelier-Lubrano, C, Spiegelman, B, Kim, JB, Ferre, P, et al. 1999. ADD1/SREBP-1c is required in the activation of hepatic lipogenic gene expression by glucose. *Mol Cell Biol* 19:3760-3768.

98. Azzout-Marniche, D, Becard, D, Guichard, C, Foretz, M, Ferre, P, and Foufelle, F. 2000. Insulin effects on sterol regulatory-element-binding protein-1c (SREBP-1c) transcriptional activity in rat hepatocytes. *Biochem J* 350 Pt 2:389-393.

99. Liang, G, Yang, J, Horton, JD, Hammer, RE, Goldstein, JL, and Brown, MS. 2002. Diminished hepatic response to fasting/refeeding and liver X receptor agonists in mice with selective deficiency of sterol regulatory element-binding protein-1c. *J Biol Chem* 277:9520-9528.

100. Eguchi, J, Wang, X, Yu, S, Kershaw, EE, Chiu, PC, Dushay, J, Estall, JL, Klein, U, Maratos-Flier, E, and Rosen, ED. Transcriptional control of adipose lipid handling by IRF4. *Cell Metab* 13:249-259.

101. Yang, J, Craddock, L, Hong, S, and Liu, ZM. 2009. AMP-activated protein kinase suppresses LXR-dependent sterol regulatory element-binding protein-1c transcription in rat hepatoma McA-RH7777 cells. *J Cell Biochem* 106:414-426.

102. Yap, F, Craddock, L, and Yang, J. Mechanism of AMPK Suppression of LXR-dependent Srebp-1c Transcription. *Int J Biol Sci* 7:645-650.

103. Zhou, G, Myers, R, Li, Y, Chen, Y, Shen, X, Fenyk-Melody, J, Wu, M, Ventre, J, Doebber, T, Fujii, N, et al. 2001. Role of AMP-activated protein kinase in mechanism of metformin action. *J Clin Invest* 108:1167-1174.

104. Cornelius, P, Marlowe, M, Lee, MD, and Pekala, PH. 1990. The growth factor-like effects of tumor necrosis factor-alpha. Stimulation of glucose transport activity and induction of glucose transporter and immediate early gene expression in 3T3-L1 preadipocytes. *J Biol Chem* 265:20506-20516.

105. Helgason, CD. 2005. Culture of primary adherent cells and a continuously

growing nonadherent cell line. *Methods Mol Biol* 290:1-12.

106. Tontonoz, P, Hu, E, and Spiegelman, BM. 1994. Stimulation of adipogenesis in fibroblasts by PPAR gamma 2, a lipid-activated transcription factor. *Cell* 79:1147-1156.

107. Swulius, MT, and Waxham, MN. 2008. Ca(2+)/calmodulin-dependent protein kinases. *Cell Mol Life Sci* 65:2637-2657.

108. Berglund, ED, Lee-Young, RS, Lustig, DG, Lynes, SE, Donahue, EP, Camacho, RC, Meredith, ME, Magnuson, MA, Charron, MJ, and Wasserman, DH. 2009. Hepatic energy state is regulated by glucagon receptor signaling in mice. *J Clin Invest* 119:2412-2422.

109. Shen, QW, Zhu, MJ, Tong, J, Ren, J, and Du, M. 2007. Ca2+/calmodulin-dependent protein kinase kinase is involved in AMP-activated protein kinase activation by alpha-lipoic acid in C2C12 myotubes. *Am J Physiol Cell Physiol* 293:C1395-1403.

110. Stahmann, N, Woods, A, Carling, D, and Heller, R. 2006. Thrombin activates AMP-activated protein kinase in endothelial cells via a pathway involving Ca2+/calmodulin-dependent protein kinase kinase beta. *Mol Cell Biol* 26:5933-5945.

111. Djouder, N, Tuerk, RD, Suter, M, Salvioni, P, Thali, RF, Scholz, R, Vaahtomeri, K, Auchli, Y, Rechsteiner, H, Brunisholz, RA, et al. PKA phosphorylates and inactivates AMPKalpha to promote efficient lipolysis.

EMBO J 29:469-481.

112. Gauthier, MS, Miyoshi, H, Souza, SC, Cacicedo, JM, Saha, AK, Greenberg, AS, and Ruderman, NB. 2008. AMP-activated protein kinase is activated as a consequence of lipolysis in the adipocyte: potential mechanism and physiological relevance. *J Biol Chem* 283:16514-16524.

113. Hurley, RL, Barre, LK, Wood, SD, Anderson, KA, Kemp, BE, Means, AR, and Witters, LA. 2006. Regulation of AMP-activated protein kinase by multisite phosphorylation in response to agents that elevate cellular cAMP. *J Biol Chem* 281:36662-36672.

114. Eberle, D, Hegarty, B, Bossard, P, Ferre, P, and Foufelle, F. 2004. SREBP transcription factors: master regulators of lipid homeostasis. *Biochimie* 86:839-848.

115. Gavin, LA, and Moeller, M. 1983. The mechanism of recovery of hepatic T4-5'-deiodinase during glucose-refeeding: role of glucagon and insulin. *Metabolism* 32:543-551.

116. Unger, RH, Eisentraut, AM, and Madison, LL. 1963. The effects of total starvation upon the levels of circulating glucagon and insulin in man. *J Clin Invest* 42:1031-1039.

117. Seidell, JC, Bjorntorp, P, Sjostrom, L, Kvist, H, and Sannerstedt, R. 1990. Visceral fat accumulation in men is positively associated with insulin, glucose, and C-peptide levels, but negatively with testosterone levels. *Metabolism*

39:897-901.

118. Stumvoll, M, Nurjhan, N, Perriello, G, Dailey, G, and Gerich, JE. 1995. Metabolic effects of metformin in non-insulin-dependent diabetes mellitus. *N Engl J Med* 333:550-554.

119. Scheen, AJ. 2003. Current management strategies for coexisting diabetes mellitus and obesity. *Drugs* 63:1165-1184.

120. Golay, A. 2008. Metformin and body weight. *Int J Obes (Lond)* 32:61-72.

121. Zang, M, Zuccollo, A, Hou, X, Nagata, D, Walsh, K, Herscovitz, H, Brecher, P, Ruderman, NB, and Cohen, RA. 2004. AMP-activated protein kinase is required for the lipid-lowering effect of metformin in insulin-resistant human HepG2 cells. *J Biol Chem* 279:47898-47905.

122. Boyle, JG, Logan, PJ, Jones, GC, Small, M, Sattar, N, Connell, JM, Cleland, SJ, and Salt, IP. AMP-activated protein kinase is activated in adipose tissue of individuals with type 2 diabetes treated with metformin: a randomised glycaemia-controlled crossover study. *Diabetologia* 54:1799-1809.

123. Caton, PW, Kieswich, J, Yaqoob, MM, Holness, MJ, and Sugden, MC. Metformin opposes impaired AMPK and SIRT1 function and deleterious changes in core clock protein expression in white adipose tissue of genetically-obese db/db mice. *Diabetes Obes Metab*.

124. Shaw, RJ, Lamia, KA, Vasquez, D, Koo, SH, Bardeesy, N, Depinho, RA, Montminy, M, and Cantley, LC. 2005. The kinase LKB1 mediates glucose

homeostasis in liver and therapeutic effects of metformin. *Science* 310:1642-1646.